NTNU

Norwegian University of
Science and Technology

In Situ Nanomechanical Testing of Electrochemical Hydrogen Permeation Membranes

A critical approach to study hydrogen embrittlement

Marte Waage Haga

Mechanical Engineering
Submission date: June 2017
Supervisor: Afrooz Barnoush, MTP

Norwegian University of Science and Technology
Department of Mechanical and Industrial Engineering

Preface

This master thesis is written at the department of Mechanical and Industrial Engineering at the Norwegian University of Science and Technology during the spring of 2017. It consists of a novel approach, using In Situ Nanoindentation to study the fundamental mechanism of hydrogen embrittlement. Based on similar research conducted by this thesis' main supervisor and his team of PhD students this new approach can be a crucial contribution to their continuous work on hydrogen embrittlement. It is closely linked to the project report written during the fall of 2016, where the custom made electrochemical hydrogen permeation cell which is used in this thesis was designed and manufactured.

I would like to express my gratitude to my main supervisor Afrooz Barnoush who always contributed with great ideas and thoughtful insight. In addition, I want to acknowledge my closest companion through this thesis, PhD Candidate Tarlan Hajilou. She gave me all the necessary training and was a vital support during my experimental work. Also the fine mechanical workshop with Øystein Hagemo have been very helpful and crucial to the development of the cell design for which I am very grateful. Lastly, I would like to like to thank my family and friends who have supported me through the entire master thesis process and have motivated me to deliver my best.

Trondheim, June 2017

Marte Waage Haga

Abstract

The purpose of this thesis is to determine if the new novel approach of investigating the effects of hydrogen, using a custom made hydrogen permeation cell together with a nanoindenter can give insight into the fundamental mechanism of hydrogen embrittlement. The sample used in this experiment is mainly an Fe3%Si sample. Similar work involving in situ nanoindentation [1, 2] and micro-cantilever bending [3] has shown changes in material behavior such as change in pop-in load and crack propagation in the presence of hydrogen. These experiments have been charging the samples by covering the indentation surface with an electrolyte and charging it as a one sided permeation cell. For this experiment the electrolyte is moved to the opposite side of the indentation surface. By doing so one can remove any contributing effect of the electrolyte on the indentation surface and only measure the effect of the hydrogen by charging the sample with hydrogen while indenting. During the fall of 2016 a custom made electrochemical cell was designed and manufactured for this purpose.

In addition to the nanoindentation, two experiments using microindentation is also performed. By indenting deeper the hydrogen concentration should be higher based on the theory of linear hydrogen concentration gradient through the sample during steady state charging[4]. Calculations based on a similar experiment done in 2015 [5] reveal that the concentration at the nanoindentation depths are very low compared to the charging surface and is the main limit of this approach. An other concern is the functionality of the cell. In order to determine if there was any hydrogen diffusing through the sample with this cell, a full permeation experiment was also conducted.

Neither the nanoindenation nor the microindentation produced any reproducible changes after the hydrogen charging. In addition to this it was found that the pop-in load can vary greatly within one grain, something that raises questing whether or not the pop-in load is a good measure of change due to hydrogen effect for Fe3%Si. The full permeation experiment gave inconclusive results about the functionality and requires further work to be determined. Based on this information it has been concluded that the hydrogen concentration at the indentation depths are too low to have an effect which can be measured with this approach, even if the cell should be proven to function. For future work an effort should be made to determine the functionality of the cell, as well as figure out how high the hydrogen concentration should be in order to measure an effect. Based on this specific experimental parameters can be determined (Sample thickness, charging current, electrolyte etc.).

Sammendrag

Målet med denne masteroppgåva er å avgjere om ein ny metode for undersøking av hydrogeneffekt, som inkluderer ei spesiallaga permeasjoncelle i samhandling med ein nanoindenter, kan gi eit nytt innblikk inn i den grunnleggande mekanismen bak hydrogensprøheit. Prøvematerialet brukt for dette arbeidet er i hovudsak Fe3%Si. Liknande arbeid med in situ nanoindentering [1, 2] og bøying av mikrobjelker [3] har gitt resultatet som tilseier ei endring i materialets respons når hydrogen er tilstade i metallet. Dette har vært endringar i blant anna «pop-in» kraft og sprekkforplantning. Ved desse eksperimenta har overflata man indenterer på vorte dekka av ein elektrolytt og prøvestykket har blitt lada som ei einsidig permeasjoncelle. For dette eksperimentet ynskjer ein å flytte elektrolytten til undersida av prøven og lade den fra undersida samtidig som man indenterer, på denne måten vil ein unngå noko effekt av elektrolytten på overflata. Dette vil kunne gje resultat som berre viser effekten av hydrogen aleine. I løpet av hausten 2016 vart cella som brukast i dette eksperimentet designa og laga til dette formålet.

I tillegg til nanoindentering blir det gjennomført to forsøk med mikroindentering. Ved å indentere djupare inn i material vil ein nå ned til ein høgare konsentrasjonen av hydrogen. Denne hypotesen er basert på teorien om den lineære gradienten til hydrogen konsentrasjon gjennom ein prøve [4] og kalkulasjonar basert på liknande permeasjonsforsøk [5] er gjennomført. Desse kalkulasjonane viser ein svært lav konsentrasjon ved nanoindenteringsdjupna samanlikna med overflata på den katodiske sida, noko som kan forklare ein manglande målbar hydrogeneffekt. Ei anna uro gjeld funksjonaliteten til sjølve cella. For å avgjere om cella fungere slik den skal og at hydrogen diffuserer gjennom prøva ved lading vart det i tillegg satt opp et permeasjonsforsøk med både anodisk og katodisk side.

Verken ved nanoindentering eller mikroindentering vart det observert nokon reproduserbare endringar grunna hydrogen effekt. I tillegg til dette vart det oppdaga at «pop-in» krafta kan endre seg drastisk basert på kvar i kornet ein oppheld seg. Dette setter spørsmål ved om «pop-in» kraft er ein parameter ein skal sjå på ved undersøking av hydrogen effekt i Fe3%Si. Permeasjonsforsøket som vart satt opp gav mangelfulle svar og det vil dermed krevje fleire forsøk for å kunne avgjere om cella fungere slik den er tiltenkt. Sett vekk frå dette har ein konkludert med at hydrogen konsentrasjonen ved indenteringsdjupna er for lav til å ha ein målbar effekt med denne tilnærminga. Basert på dette vil vidare arbeid bestå av først å avgjere om cella fungere med fleire testar og deretter avgjere kva hydrogenkonsentrasjon som vil være kritisk for å kunne måle ein effekt, og på grunnlag av dette kan ein gjennomføre forsøk med parameterar (prøvetjukkelse, elektrolytt, potensial og strøm) som oppfyller hydrogenkonsentrasjonskriteriet.

Contents

List of Figures

List of Tables

Abbreviations

BCC	Body Centered Cubic
DS	Devanathan-Stechurski
EDS	Energy Dispersive Spectroscopy
EHAC	Environmental Hydrogen Assisted Cracking
EHPC	Electrochemical Hydrogen Permeation Cell
FCC	Face Centered Cubic
HCP	Hexagonal Close Packed
HDN	Homogeneous Dislocation Density
HE	Hydrogen Embrittlement
HEDE	Hydrogen Enhanced Decohesion
HELP	Hydrogen Enhanced Local Plasticity
IHAC	Internal Hydrogen Assisted Cracking
NI-AFM	Nanoindentation with Atomic force microscopy
SDSS	Super Duplex Stainless Steel
SEM	Scanning Electron Microscope
SFE	Stacking Fault Energy
UTS	Ultimate Tensile Stress

Nomenclature

C_0	Sub-surface hydrogen concentration at the charging side [ppm W]
C_{avg}	Average hydrogen concentration in sample [ppm W]
C_x	Hydrogen concentration at the indentation depth [ppm W]
L	Thickness of sample [m]
X	Indentation Depth [m]
μ	Shear Modulus [Pa]
ρ	Dislocation Core Radius [m]
γ	Stacking Fault Energy $[mJm^{-2}]$
D_{eff}	Effective Diffusion Coefficient $[m^2s^{-1}]$

1 Introduction

The phenomenon of hydrogen embrittlement (HE) was discovered already in 1875 by William Johnson [7]. Since then the phenomenon has been greatly researched resulting in an abundance of theories and proposals for the mechanism which leads to hydrogen embrittlement. Regardless of this, no single mechanism has been agreed upon. As seen in figure 1 hydrogen embrittlement needs three aspects in order to take place.

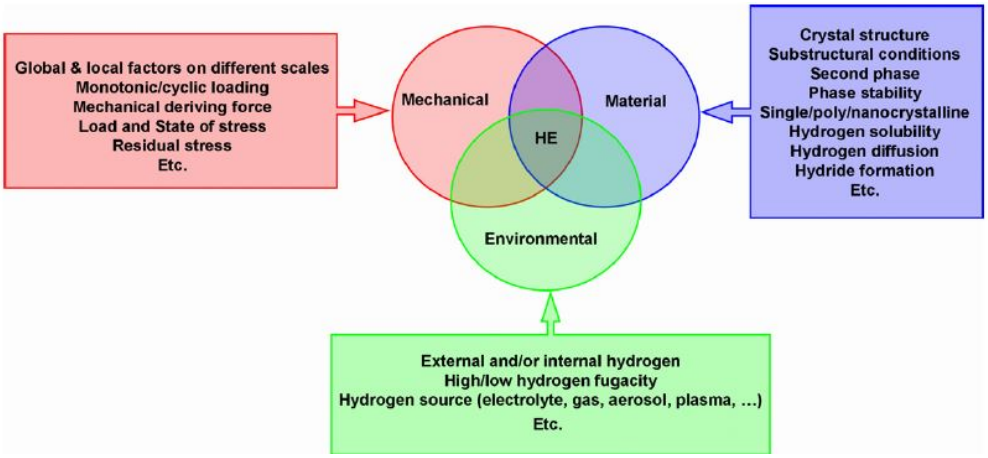

Figure 1: The three aspects of hydrogen embrittlement

Based on the graphical presentation of the phenomenon it is evident that it is complex and thereby highly difficult to investigate to ensure only the effect of hydrogen is measured. New research approaches allowing investigation of the phenomenon at smaller scales and in more controlled environments have enabled new insight to the effect hydrogen have on materials [1]. An example of this is nanoindentation. The main advantage of the nanoindentation technique is its capability to resolve the dislocation nucleation in samples with low dislocation density. In addition to this the mechanical aspects can be defined by using analytical solutions for stress under the indentation tip prior to dislocation nucleation. The material aspect is also resolved for this approach due to the extremely small volume being tested which can be characterized by means of techniques such as electron backscatter diffraction and electron channeling contrast. Although nanoindentation allows for a more controlled experimental approach there has in later years been developed an even more complex approach. In situ electrochemical nanoindentation enables control of environmental aspects such as hydrogen concentration. This can be done by setting the surface electrochemical potential inside an electrolyte and thereby keeping the surface hydrogen concentration constant [6, 2]. This approach, with addition of in situ electrochemical micro-cantilever

bending tests [3] has contributed to supporting a novel concept to describe hydrogen embrittlement both through analytic calculations and experimental results. The concept tries to explain the underlying mechanisms leading to the interpretation of HEDE and HELP. This concept has been called defactant concept and will be explained in more detail later.

For this master thesis the in situ nanoindentation approach used in the experiment described above will be further developed with a new electrochemical setup allowing indentation on a surface which is not covered by electrolyte. Based on this it can be discovered if the presence of electrolyte plays a role in the interpretation of results or if it is the hydrogen which actively contributes to the observed changes in pop-in loads and crack propagation. The main objective of the experimental work is to determine if this new approach can increase insight into the fundamental hydrogen embrittlement mechanism. The initial plan is to test simple ferritic steels with different diffusion rate and solubility and determine what types of changes one can observe. This can thereby be compared to experiments where similar or different changes have been observed. Since this cell is the first of its kind, further development of the cell itself will be a equally important factor during the project scope.

The thesis will firstly describe some relevant theory before the experimental setup is presented. Since this project work is continually developing the experimental procedure, together with results and a discussion and conclusion, is described for each individual test. Based on the contents of the tests a conclusion is made and further work is proposed.

2 Theory and Previous Research

In order to understand the underlying theory which has been used in order to perform the intended experimental research and ensure an in depth discussion of experimental results necessary theory and previous research has to be explored. For this thesis both hydrogen related topics in addition to the theory of testing procedures have to be described. This chapter will describe the behavior of hydrogen related to hydrogen evolution, diffusion and trapping. The suggested mechanisms of hydrogen embrittlement will be presented, as well as the two main testing methods which are relevant for the thesis, micro hardness testing and nanoindentation with accompanying data interpretation and phenomena.

2.1 Hydrogen

Hydrogen is not only the most common element in the universe it is also the lightest with its single proton and electron in its electrically neutral atom state. It has the ability to diffuse into metals and alloys. This phenomenon has been found to be both beneficial for hydrogen storage solutions [8] and catastrophic for oil and gas equipment such as pipelines [9]. The latter is often related to hydrogen embrittlement, the hydrogen induced degradation of metals which cause severe problems, but is yet to be fully understood regardless of extensive research [3].

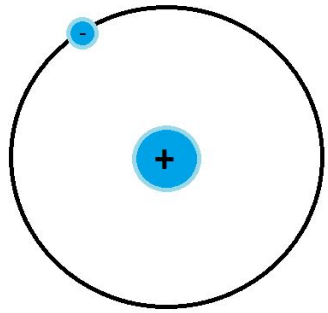

Figure 2: Hydrogen atom in electrically neutral state

2.1.1 Hydrogen Evolution

The kinetics of generation of hydrogen is different for gaseous and aqueous media [10]. The reduction reactions at the metal-solution interface in aqueous solution is illustrated in figure 3

and will be the relevant reactions for this thesis. The predominant reaction for cathodic reduction reactions involves both protons H^+ and water H_2O as seen to the left in the figure. For sour environments, like the ones found on offshore pipelines, also reduction of H_2S can occur, and has to be considered as an additional process. For the hydrogen evolution there are two processes, namely chemical recombination (Tafel reaction) of absorbed hydrogen atoms as seen to the left in the figure and electrochemical recombination (Heyrovsky reaction) involving both the absorbed hydrogen and the proton as seen to the right.

Water Reduction Reaction:

$$(a) \quad 2H_2O + 2e^- \rightarrow H_2 + 2OH^- \quad (In\ alkaline\ solutions) \tag{1}$$

$$(b) \quad 2H_3O + 2e^- \rightarrow H_2 + 2H_2O \quad (In\ acid\ solutions) \tag{2}$$

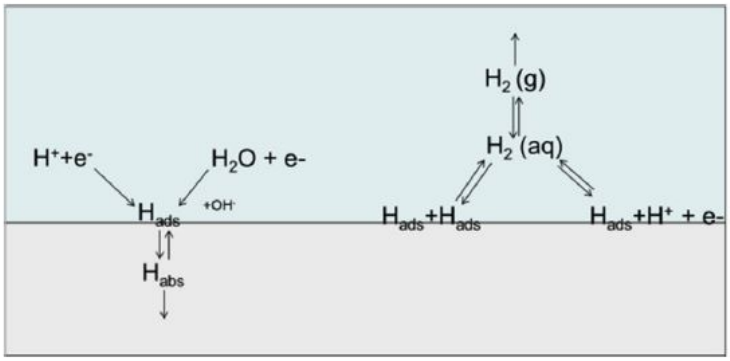

Figure 3: Reaction Process at Charging Surface

2.1.2 Hydrogen Solubility and Diffusivity

Some metals are more susceptible to hydrogen diffusion and this is determined by the effective solubility of hydrogen in the metal [11]. There are several factors affecting the solubility, such as the nature of the surface, presence of oxide layer, lattice and microstructural trap sites. The main mechanism hydrogen diffusion in steel is interstitial jumps in the metal lattice. Based on this a simplified overview of the diffusion rate and related solubility is given in the table below with respect to the crystal structure present in the metal. The table shows that the BCC structure,

which is ferritic, has a high diffusion rate, which is due to its open lattice structure. It is important to note that though this table can give a good indication of diffusion and solubility it does not take into account all the influencing factors.

	BCC (Ferrite)	BCT, HCP (Martensite)	FCC (Austenite)
Diffusion Rate	High	Medium	Low
Solubility	Low	Medium	High

2.1.3 Hydrogen Permeation and Trapping

The sources of hydrogen are many and can lead to either environmental hydrogen assisted cracking (EHAC) where the hydrogen is introduced through the surrounding environment like in cathodic protection or internal hydrogen assisted cracking (IHAC) where atomic H is introduced through the manufacturing process such as welding, electroplating and electric discharge [3, 10]. In order for the hydrogen to diffuse through a metal the atoms needs to hop or quantum tunnel between interstitial sites. If the concentration of molecular hydrogen in solution exceeds the solubility limit then hydrogen gas bubbles will tend to form. Through the diffusion process some of the hydrogen becomes trapped inside the microstructural trap sites in the metal. These trap sites can be dislocations, grain boundaries, vacancies and interfaces and can vary in both density and distribution. Based on their binding energy the trap sites are classified as shallow or deep in relation to the specific microstructural features [12]. The permeation rate is mainly limited by either the diffusion mechanism for high permeation rates and high upstream pressure or surface process for low permeation rates and low upstream pressure [13].

In order to determine the hydrogen diffusivity through metal or alloy membranes the Devanathan-Stechurski (DS) permeation technique is commonly used. The technique consists of fixing a metal sample between two independent electrochemical cells. Each cell includes a counter-, reference- and working electrode creating a charging cell which behaves as a cathodic cell and an oxidizing cell which becomes the anodic cell based on each individual potential. The reference electrode is placed close to the working electrode to avoid voltage drop due to the solution resistance, but without obstructing mass flow to and from the working electrode. In electrochemical permeation experiments, the entry of hydrogen is controlled by the electrolyte and the applied cathodic polarization potential. The hydrogen ions (H^+) are produced on the cathodic side and are absorbed on the sample surface before they diffuse through the metal sample. On the anodic side the hydrogen ions are oxidized. The anodic side is polarized to the hydrogen equilibrium potential. In some cases a thin coat of palladium is used as a catalyst for the hydrogen oxidation to resolve hydrogen transport. Figure 4 below illustrates a typical DS cell, with additional nitrogen inlet for oxygen

removal[14].

On the anodic side of the permeation cell the hydrogen undergoes hydrogen recombination, this is the opposite reaction to the hydrogen evolution found on the cathodic side. It is important to note that the recombination reaction can also be found on the cathodic side during charging. The desorption kinetics of the hydrogen can be described by the chemical recombination (Tafel reaction):

$$H_{ads} + H_{abs} \rightarrow H_2 \tag{3}$$

or the Heyrovsky reaction:

$$H_{ads} + H^+ + e \rightarrow H_2 \tag{4}$$

The recombination reactions can be reduced or prevented, by the presence of an oxide layer or more actively, by use of cathodic poisons, enhancing hydrogen entry into metallic materials. The most common poision is H_2S, but also other anions such as phosphate, sulfate and nitrate can be used [15].

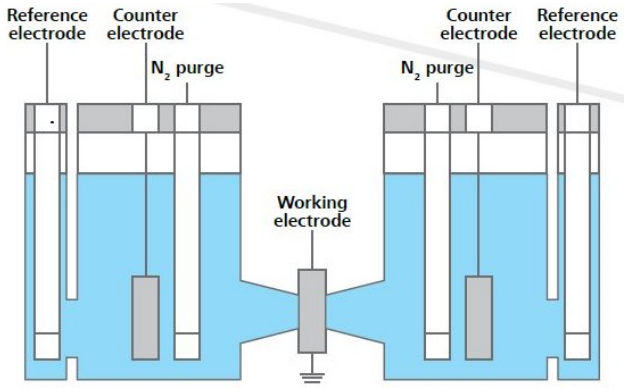

Figure 4: Devanathan-Stechurski permeation cell

The hydrogen diffusion coefficient and the concentration of hydrogen can be found based on the permeation technique. There are several approaches, such as breakthrough time t_b, the elapsed time t_{lag} and the slope method. The equations for calculations the different parameters can be found in the ASTM standards [16].

It is assumed that the sub surface concentration on the charging side is constant during steady state charging. For these conditions also the concentration on the anodic side, due to oxidation is assumed to be zero. Since the diffusion coefficient is not affected by the concentration the distribution of diffusible hydrogen inside the sample can be described as a liner gradient as shown in figure 5. This average steady state diffusible hydrogen can be expressed as a charge using equation (5) [4]

$$C_{avg} = \frac{C_0 * L}{2} \tag{5}$$

Where C_o is the concentration at the charging side and L is the thickness of the sample. To find a concentration anywhere in the sample, the equation can be expressed like this:

$$C_x = \frac{C_0 * X}{L} \tag{6}$$

where X is the distance from the anodic side, into the sample. These concentrations however are only the diffusible hydrogen in the lattice. If there is hydrogen trapped in the material, and additional concentration of trapped hydrogen will have to be added [4].

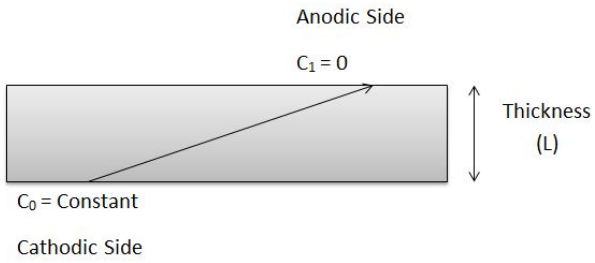

Figure 5: Hydrogen concentration gradient in finite slab

2.2 Mechanisms of Hydrogen Embrittlement

Despite of the continuous research to find the mechanism of hydrogen embrittlement, there are still multiple theories and proposals which are highly disputed. Some of the theories are more referenced than others where Hydrogen Enhanced Local Plasticity, Hydrogen Enhanced Decohesion and Hydride Formation and Cleavage range at the top. More recently new concepts have been proposed, such as the thermodynamic defactant concept. This chapter will describe in more detail what these theories and concepts include.

2.2.1 Hydrogen Enhanced Local Plasticity

Hydrogen enhanced localized plasticity (HELP) is primarily supported through experimental observations of enhanced dislocation movement in the presence of hydrogen, as well as the localized slip-bands in the local area of the crack tip [17]. In order for HELP to initiate there are two main mechanisms. These are 1) increased dislocation mobility, which leads to material softening and 2) reduced dislocation-dislocation interactions due to hydrogen. This reduction enables planar slip and increase pile-up phenomena that can lead to damage initiation.

2.2.2 Hydrogen Enhanced Decohesion

The model of Hydrogen Enhanced Decohesion (HEDE) is based on the decrease of cohesive force due to solute hydrogen. The presence of hydrogen atoms is assumed to lower the surface energy of atomic planes or grain boundaries and thereby encouraging more cleavage-like failures[18]. The dislocation density increases when subjected to pre-strain, thereby increasing the ultimate tensile stress (UTS), but it has been found that HEDE is constantly in competition with strain hardening and that high pre-strain lead to HEDE being dominant and therefore decreasing the UTS when hydrogen is present. For this mechanism the local concentration play a significant role, where high concentration can lead to lower resistance to HE (Hydrogen Embrittlement) [17].

2.2.3 Hydride Formation and Cleavage

This mechanism is particularly applicable to hydride forming systems and consists of brittle hydride precipitates forming in the material causing embrittlement. There has also been observations of the phenomena in other materials that undergo hydrogen embrittlement [19].

2.2.4 Defactant Concept

Based on recent studies a new concept called defactant concept and decohesion have been fund to successfully describe hydrogen embrittlement [6]. The concept describes hydrogen embrittlement (HE) as a decrease in the defect formation energy and based on the experimental approach the results can be interpreted as Hydrogen Enhanced Local Plasticity (HELP) and Hydrogen Enhanced Decohesion (HEDE).

The name of the concept arises from DEFect ACTing AgeNTS (Defactants), and is a term covering the action of atoms segregating to defects in solids and reducing their formation energy similarly to the way that surfactants reduce surface energies in liquids. In the case for hydrogen embrittlement these defactants are solute hydrogen in the lattice. In any material there is something called the activation energy of homogeneous dislocation nucleation (HDN) which is related to the material specific parameters shear modulus μ, dislocation core-radius ρ and stacking fault energy (SFE) γ. For a material without dislocations the indentation will progress elastically until the theoretical shear strength is reached under the tip. At this point dislocations will homogeneously nucleate, followed by subsequent glide and multiplication events, hence the name homogeneous dislocation nucleation.

Through experiments it was discovered that the hydrogen reduced the activation energy for HDN through the effect on the parameters mentioned. For example local reduction in the shear modulus was found when a small volume strained lattice was enriched with hydrogen. This was found to be enough to reduce the activation energy for dislocation nucleation. Also the interatomic binding forces and the dislocation line energy within the dislocation core can be affected by the hydrogen as well as the SFE in the case on partial dislocations in FCC crystals. Thus, the process of hydrogen embrittlement is controlled by a decrease in the defect formation energy and a reduction in the interatomic bonding energy.

2.3 Mechanical Testing

There are several methods to determine the mechanical properties of a material. This can be done for example through the classic tensile and compression test, bending and torsion test, or like this thesis will show, through hardness testing. Just within the field of hardness testing there are multiple approaches and methods which can be applied. This thesis will only focus on the approaches which have been used, namely Vickers hardness test and nanoindentation.

2.3.1 Vickers Hardness Test

The Vickers Hardness Test [20] is a method to measure the hardness of materials and was developed in 1921 by Robert L. Smith and George E. Sandland. The method is an alternative to the Brinell and Rockwell method and the specific method gives an unique output, like Brinell-, Rockwell- or Vickers Hardness. The main difference is the indenter tip. For Vickers hardness testing a square based pyramidal diamond indenter is used, this does not deform during indentations, enabling reliable indention results, even on hard materials. ISO 6507 [21] describes the specific procedure and parameters in order to execute a proper hardness measurement with the Vickers method.

The hardness is calculated using equation (7) based on the indentation diagonal (d) measured after indentation and applied force (F). The measure of the diagonal can be seen in figure 6 and is also given in equation (8).

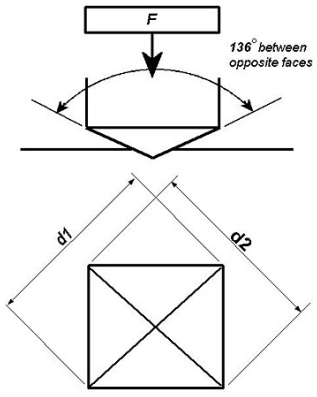

Figure 6: The Schematics of the Vickers Indenter Hardness Measurement

$$HV = \frac{0.1891F}{d^2} \tag{7}$$

$$d = \frac{d_1 + d_2}{2} \tag{8}$$

$$h = \frac{d}{2\sqrt{2}\tan(\Theta/2)} \tag{9}$$

$$h = \frac{d}{7.0006} \tag{10}$$

In addition to the diagonal and hardness the indentation depth can be of interest, for this measure equation (9) can be used. Where Θ is the angle between to opposite faces and d is the diagonal of the impression. The HM-210/220 Series 810- Micro Vickers Hardness Testing Machines delivered by Mitutoyo produce a hardness value directly based on the manual measurements made by the dual line filar eye piece, but does not give an output on the depth of the impression. The specifics on how to operate the machine can be found in the user manual [22].

2.3.2 Nanoindentation

For testing of materials at nanoscale, nanoindentation is most commonly used. Compared to microscale, the extremely small dimension presents high surface proportions, less defectives and unique properties [23]. For hydrogen embrittlement nanoindentation has become an increasingly used approach. Nanoindentation allows for local examination of the hydrogen effect by reducing the scale of the testing method down to the microstructural level [6]. Nanoindentation was introduces in the 1970's and aims at measuring the hardness of a material through indenting the subsurface of a test sample. The indentation method can be regarded as non-destructive, due to the shallow indentation depth and the small indenter probe radius. The method provides information about the elastic modulus, hardness, strain-hardening, cracking, phase transformations, creep, and energy absorption based on load-displacement calculations and analysis of the curve shape. The load and displacement are monitored and the area of contact is determined by the depth of the impression and the known angle or radius of the indenter. One can use several different indenter probes such as Berkovich, conical, spherical or Vickers and custom load functions. The tip used for this thesis will be Berkovich, a fairly sharp indenter tip with a face angle of 63.5° as seen in figure 7. The advantage of this tip is its sharp and well defined tip-geometry, as well as it has a well-defined plastic deformation into the surface and is good for measuring modulus and hardness values. The main disadvantage with this tip is the unclear elastic-plastic transition [23].

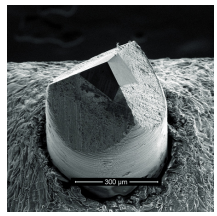

Figure 7: Berkovich indentation probe tip

2.3.2.1 Factors Affecting Nanoindentation Results

There are several factors which affect nanoindentation results [23]:

- Thermal drift: Change in dimensions of the instrument due to thermal expansion or contraction of the apparatus can cause a drift in the indentation data which is observed as a change in depth, with constant load. It can be computed by reading depth change over time and based on that, adjustments can be made accordingly.

- Initial Penetration Depth: In order for the nanoindenter to be able to start measuring, the

tip will have to make actual contact with the sample surface. This contact depth is made as small as possible, often an initial contact force of 1μm is enough. However, since the penetration does occur, it needs to be accounted for in the analysis of the indentation curve. Whether or not the response to this contact is elastic or plastic is dependent on the indenter tip used.

- Instrumental Compliance: For nanoindentation the response from both the sample and the instrument used is measured. Usually the instrument includes the compliance of the instrument in its measurement using a compliance factor including the compliance of the loading frame, the indenter shaft, and the specimen mount. This factor is usually found through experimental approaches.

- Indenter Geometry: Since the area of contact for nanoindentation is found through the indenter tip geometry it assumes an ideal shape. This is however impossible to achieve in practice. To counter this, specific correction factors are applied to find the real area. These correction factors are found by direct measurements, or more often, an indirect method including a series of indentations at varying maximum loads on standard test specimens.

- Piling-up and Sinking-in: Piling-up and sinking-in are two common responses to the contact between the specimen surface and the indentation tip. The latter is typically found in elastic materials where the surface of the specimen can often be drawn inward and downward. In the cases where the contact involves plastic deformation, both sinking-in and piling-up can be included and the degree depends upon the ratio E/Y and the strain-hardening properties. In the case of pile-up and sinking-in the true contact area can vary greatly from the calculated area, resulting in inaccurate results. There have been proposed several methods to account for this effect.

- Indentation Size Effect: Although one would expect that for a homogeneous, isotropic material the measure of hardness and modulus would be limited to one value, it actually can be affected by the indentation depth. This is known as the indentation size effect and should not be confused with actual real reflections of material behavior due to for example an oxide layer, residual stress or strain-hardening due to preparation. For hard materials, very little indentation size effect is expected. For soft material, and especially crystalline materials, a significant indentation size effect is expected.

- Surface Roughness: Similar to the indentation tip geometry, the surface roughness of a specimen is not ideal. In general, surface roughness is characterized by the asperity height and the spatial distribution of them across the surface. The effect of the surface roughness

depends on the indenter tip. For blunt tips with low load such as the spherical tip the effect is much higher than for sharp tips such as the Berkovich tip.

- Tip Rounding: Indenter tips such as the Berkovich is not perfectly sharp, but actually has a tip radius in the order of 100nm. The effect of this rounding is most critical for indentation on thin films less than 500nm thickness and maximum penetration depth of 50nm. The rounding causes an initial elastic contact, resulting in hardness measurement error since the mean contact pressure may no reflect the conditions of a fully formed plastic zone. To counter this, the real indenter could be modeled as a sphero-conical indenter. It is however important to note that more recent work has indicated that the tip radius is not a good measure of merit for the effectiveness of a sharp indenter and the concept of plastic depth has been introduced to describe the suitability of an indenter more realistically. Since the indentation depth for this thesis will be in the order of 200nm and the samples are in the 1mm range this effect is not further discussed.

- Residual Stress: After processing or surface preparations many material experience stresses, both tensile and compressive. These stresses are known as residual stress and can influence the nanoindentation results. How the residual stress effect the hardness measurements vary from material and experiment, and between bulk and thin film specimens and one conclusive effect is difficult to specify.

- Friction and Adhesion: Nanoindentation is associated with small loads and displacements. On that basis it would be reasonable to wonder if the surface forces have any effect on the contact mechanics and thereby the computed material properties. It has been found that the adhesive force is significant for very compliant surfaces even when the contacts are large. This is however most significant for loads in the pN-nN regime and thereby not for this thesis as the load are in the *mu*N regime.

- Specimen Preparation: The specimen preparation is closely linked to both the surface roughness, as well as the residual stress effect. For nanoindentation a 1μm polishing compound gives a good mirror finish. This is accomplished by carefully polishing with a decreasing grit size and thorough washing. A by-product of this polishing is strain-hardening or cold-working and is especially a concern for metals. This could lead to unwanted indentation size effect. To overcome this effect an indentation depth above the nominal grit size is deemed necessary. For indentation depths below this, one can expect change in material properties.

2.3.2.2 Nanoindentation Data and Phenomenons

The principal goal of nanoindentation is to extract the elastic modulus and hardness of the material. Indentation modulus is not the same as the elastic modulus for all materials due to the effect of material behavior such as pile-up. After the indentation is conducted a force-displacement curve is generated based on the force applied to the indentation probe and the indentation depth. The indenter can be programmed to be load or displacement controlled based on the desired result. Based on the material's response and properties, the load-displacement curves can vary in shape. Figure 9 illustrates some examples of this.

The pop-in event as shown for the Sapphire in figure 9 (d) is a phenomenon of rapid depth change often associated with the onset of plastic deformation. The phenomenon can be caused by deformation mechanisms such as phase change[24] or homogeneous dislocation nucleation [25]. It has been found that hydrogen charging clearly reduces the pop-in loads for Fi3%Si through in-situ electrochemical nanoindentation [26]. This new approach using nanoindentation, combined with the novel thermodynamic defactant concept has given new insight into the mechanism of hydrogen embrittlement.

2.3.2.3 In Situ Electrochemical Nanoindentation

In-situ electrochemical nanoindentation is a fairly new approach to investigate hydrogen embrittlement. Since the experimental method of studying hydrogen embrittlement is based on elimination of diverse factors within mechanical, material and environmental aspects [6] and the use of external stimuli can result in misinterpretation of defects, in-situ experiments are deemed necessary. A. Barnoush [27] presented a proposal novel setup for probing HE with NI-AFM on in-situ hydrogen-charged samples under controlled electrochemical conditions in 2008. This method is mainly developed to study hydrogen deformation interaction, examining the dependence of the pop-in loads on hydrogen charging and is the basis of this thesis alongside similar work [1, 6, 26, 3]. The approaches has so far focused on a custom made permeation cell where the specimen is covered by an electrolyte and nanoindentation or micro-cantilever bending has been performed in situ. The schematics can be seen in figure 8 and give a good idea of the cell setup. The next step in this experimental approach has been evaluated to be charging from underneath. Removing any effect of the electrolyte on the surface and ensuring only the hydrogen effect is measured.

Based on this it should also be possible to use the Vickers hardness test under similar conditions to investigate a possible change in hardness due to hydrogen charging, an "in-situ electrochemical Vickers hardness test".

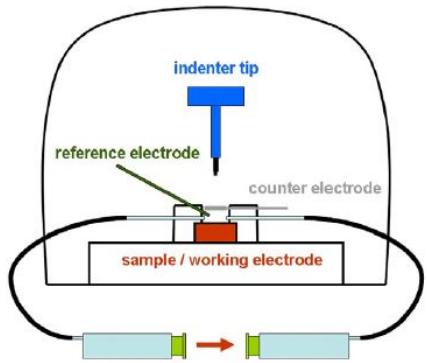

Figure 8: Schematic drawing of experimental setup [6]

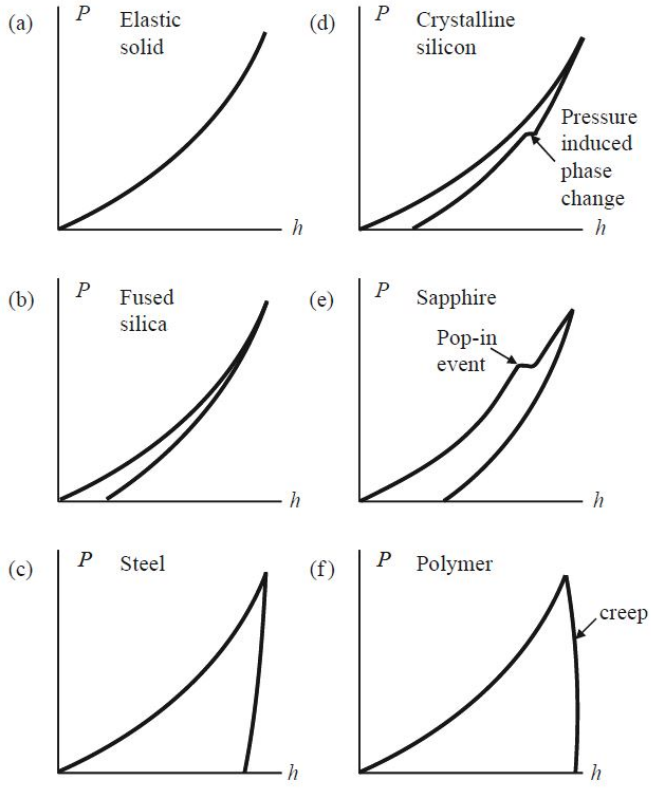

Figure 9: Different nanoindentation response in materials

3 Experimental Setup and Equipment

To ensure the reproducibility of this experimental research the description of the equipment, apparatus and setup is introduced. This includes design limitations and changes made to the design. Through the testing process described in the next chapter, several small changes were made. These respective changes will be introduced there. In addition to the equipment used, descriptions of the samples which have been used are introduced together with the sample preparation.

3.1 Electrochemical Hydrogen Permeation Cell

A specially designed electrochemical hydrogen permeation cell (EHPC) for use in the Hysitron Triboindenter was manufactured during the fall of 2016. This cell allows for in situ nanoindentation of 12mm circular samples of different materials. The EHPC is designed on the basis of the Devanathan and Stachursky method [28], but is modified for use inside the Hysitron Triboindenter. The electrochemical cell setup inside the nanoindenter is schematically illustrated by figure 10. The main and top part of the cell is made of Polychlorotrifluoroethylene (PCTFE), also known as Kel-F. The bottom part is made of plexiglass to allow inside view, which is accompanied by a stage custom made to fit inside the triboindenter. The inside view is illustrated in figure 12 b. Detailed information about the design can be found in the design report [29].

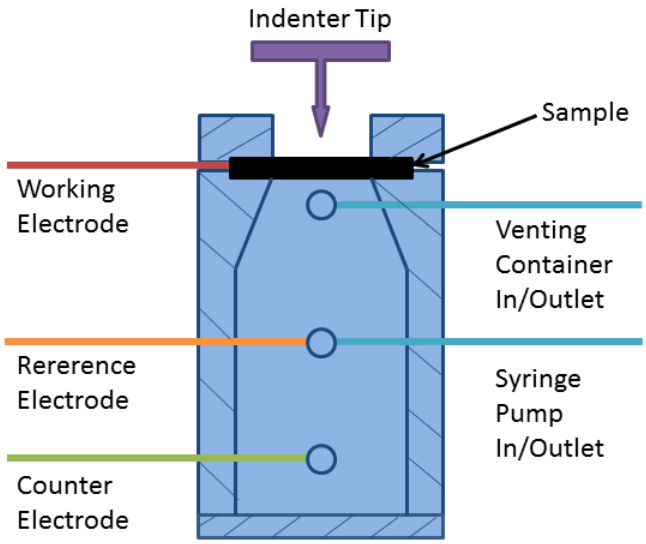

Figure 10: Electrochemical Cell Setup

The Reference Electrode used in this experimental setup is a double junction $Hg/HgSO_4$ reference electrode. This will imply that all electrochemical potentials will be referenced against an Hg/Hg2SO4 reference electrode. This specific electrode is chosen to avoid any Cl ion contamination of the electrolyte [26].

The Counter Electrode changes through the course of this experimental work from a coil of platinum wire to the custom made platinised titanium rod which is explained in more detail in 3.2.1

The Working Electrode also changes slightly through the experimental work to improve endurance. The first edition is an aluminum clamp, replaced by copper after a fracture incident in test 6.

The Electrolyte used for the charging is a glycerin ($C_3H_8O_3$) borax ($Na_2B_4O_710H_2O$) diluted with 20% or 50% distilled water electrolyte. The amount of distilled water is chosen on the basis of desired conductivity and viscosity. The advantage of this electrolyte is its extremely low solubility and diffusivity for oxygen and should allow for long time charging without effecting the sample surface [26].

The Syringe Pump which is introduced in test 2 is a LEGATO™ 270 syringe pump. This is a dual syringe, programmable touch, continuous flow, push-pull pump which replaces manual flow injections for hydrogen removal on the sample surface. The pump is used to ensure the hydrogen concentration on the charging side of sample does not exceed the limit in which the current can be kept stable. The pump is connected to the EHPC and can both inject and withdraw electrolyte to and from the cell respectively. In addition to the pump, a venting system is attached to the cell through a tube. The venting system consists of a container of electrolyte where the excess electrolyte which has been injected from the syringe pump through the cell can be stored. The hydrogen bubbles which have been removed from the cell will also be transported here through the injection step. Due to the nature of the container with an open cap the bubbles can easily escape into the free air before the withdrawal process is initiated which draws electrolyte from the venting container through the cell and into the syringe in the syringe pump. the schematic illustration of the venting system can be found in figure 11 and the process of implementing the pump can be found in more detailed in test 4.2.

The manual injection and withdrawal which had to be performed before the syringe pump arrived can be seen in figure 12 a, this figure also shows the early electrical connections in more detail.

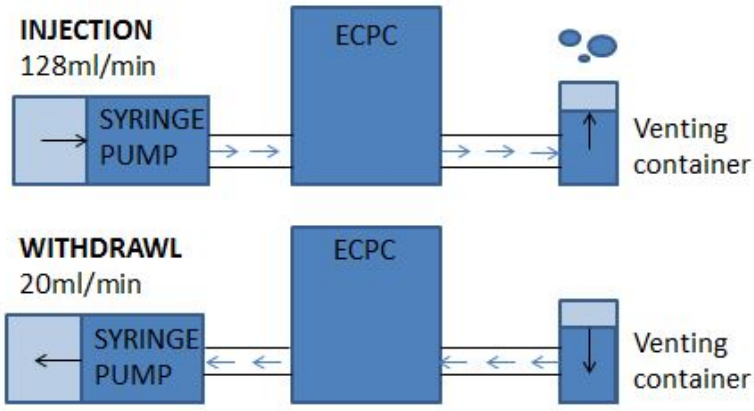

Figure 11: Schematic drawing of syringe pump setup

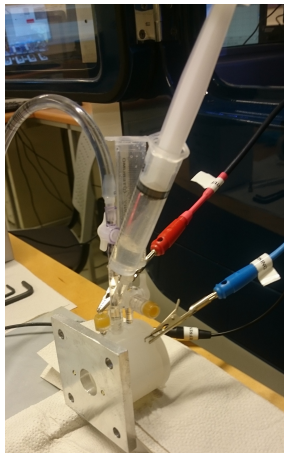

(a) Permeation cell electrical and electrolyte connections

(b) View of platinum wire counter electrode inside cell

Figure 12: Experimental setup for manual injections

Additional Apparatus to the custom made EHPC is necessary. For the nanoindentations Hysitron TI 950 TriboIndenter is used. The charging for these tests are controlled by PGU-1A-OEM-MO potentiostat monitored through ECM WIN softwear. For microindentation Mitutoyo HM-210/220 Series 810- Micro Vickers Hardness Testing Machines is used. The charging for these tests is controlled by Gamry Reference 600 potentiostat.

The Load Function for most of the nanoindentations is inspired by similar work [2] and the only parameter which has been changed in between the different tests is the maximum load. This can be clearly seen in the nanoindentation results later. The main load curve consists of a loading rate of 200002 μN/s up to the max load of 5000 μN. The max load is kept constant for 0.25 s followed by a reduction to 10% of the maximum load which is kept for 0.25 s for drift correction. The feedback during the testing was set to open-loop (no feedback) in order to control the load or the displacement during the testing. The load curve can be seen in figure 13.

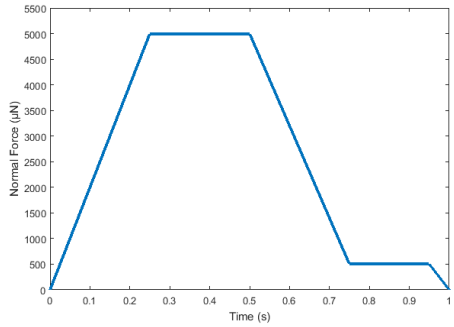

Figure 13: General load function for this thesis work

3.2 Design Limitations and Improvements

Although the EHPC described in the setup is based on the Devanathan and Stachursky method it does deviate from the original design due to the application and surroundings. The biggest difference, especially for this generation prototype is the lack of an anodic side during charging. The anodic/oxidizing side of the cell enables measurement of hydrogen diffusion. By measuring the hydrogen content on both sides the amount of hydrogen which has diffused trough the sample can be found. Without this option, the hydrogen concentration on the anodic side is hard to determine.

Since the EHPC is a prototype, there are still features in addition to the anodic side which can be improved. During the tests introduced later in this chapter some of these features are identified and measures to make improvements are implemented based on this to obtain more reliable results. The counter electrode and a new anodic top part are some of these improvements.

3.2.1 Counter Electrode

The counter electrode was one of the main problems with the cell setup, causing the cell to leak and absorb air from the surrounding during withdrawal of the syringe pump. The platinum wire which was pulled through a male luer connection with a rubber membrane started to leak after being used multiple times. To fix this, a custom made counter electrode, see figure 14, was made of platinised titanium. The electrode design included a 40mm rod, which was cut to fit into the counter electrode inlet, and threaded to ensure a sealed connection to the main cell.

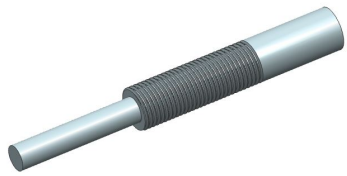

Figure 14: New Counter Electrode

3.3 Sample and Preparation

The samples have the dimensions 12mm diameter and 400μm-2mm thickness and the materials used are given in table 1. The thickness needs to be at least 10 times the indentation depth to fit the rule of thumb for nanoindentation standards and minimize the influence of the substrate [23]. For the microindentation on metallic materials the thickness should be at least 1.5 times the diagonal [30].

Table 1: Material overview

Material	Structure	Phase
Fe-3 wt.% Si	BCC	Ferrite (α)
SDSS	BCC and FCC	Ferrite (α) and Austenite (γ)
316 SS	FCC	Austenite (γ)
Zircaloy-2	HCP matrix and FCC hydrides	HCP phase (κ) and Ferrite (α)

In order to prepare these small samples for electrochemical nanoindentation they first needs to be mechanically polished. The polishing process involves grinding with a coarse (Grit 1000) polishing paper, and stepwise using finer paper (Grit 2000-4000) which is applied 90 degrees to the direction of the previous. The desired result is a surface with one directional marks from the finest paper. A combination of ethanol and water can be used during the polishing to avoid corrosion in the process. The sample surface is examined in microscope to ensure satisfactory results. After this step it is possible to move on to diamond polishing or directly to electrochemical polishing. The electrochemical polishing is performed using an electropolisher (LectroPol-5) and a custom electrolyte made of Methanol 947ml/L and H_2SO_4 53ml/L. The surface is oxidized for a certain amount of time based on the roughness of the surface and the intended result, the specific parameters which have been used is based on previous similar work [1]. After the process the samples are cleaned thoroughly with ethanol and ultrasound bath.

To achieve samples with thickness below 1mm long time electropolishing is used. A unique sample holder is utilized to specify the 2-3mm^2 area in which the thinning should be performed. The thinning is contained to a small area to avoid the large forces acting on the outer edges of the sample during the assembly of the cell to cause stress above the yield and tensile strength of the material. This can cause deformations or in worst case fracture of the sample and should be avoided. By electropolishing the contained area for a total amount of time of one hour the thickness should reduce the sample thickness in the middle from 1mm to approximately 400μm. To measure the thickness a confocal microscope can be used. This apparatus enables 3D scanning

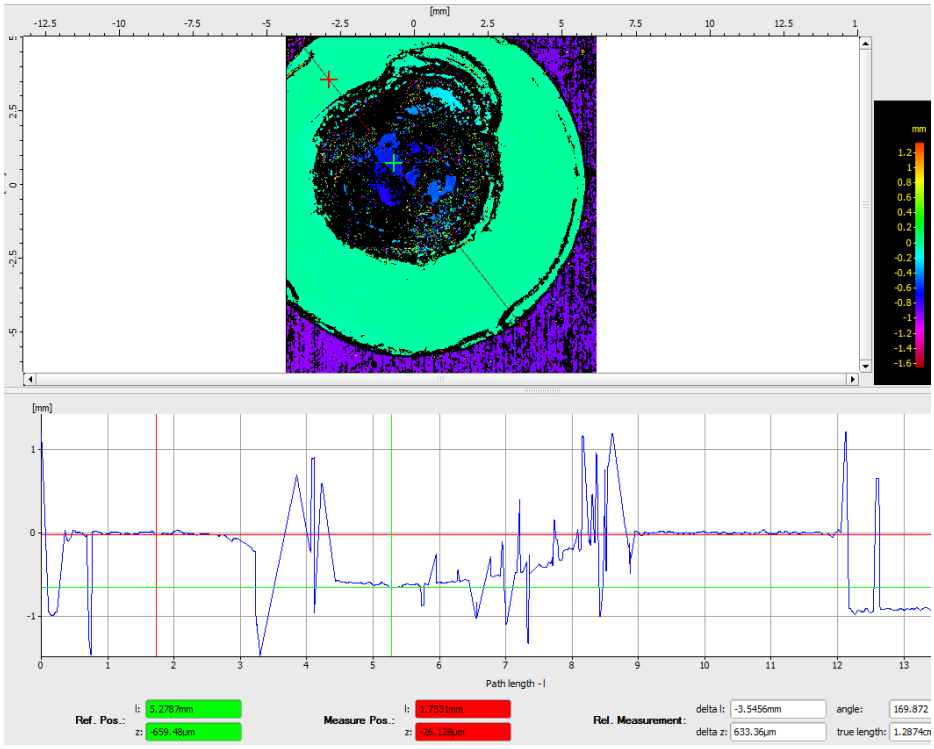

Figure 15: Characterization of thinned sample with confocal microscope

of the surface and can give a good approximation of the thickness as seen in figure 15. The colors specify the depth, where the green color on the edges is zero, and the blue parts in the middle are around -0.6mm. Since the initial thickness of the sample is known to be 1mm, the depth of the electroplished area gives the remaining thickness, in this case 400μm. The graph with the blue lines underneath the sample figure also gives a graphical profile of the sample surface where the edges can be seen between 0-3 and 9-12. Due to the shiny finish on the sample as a result of the electropolishing the microscope has problems reflecting all of the surface. This can be seen in the black areas in the sample figure and as noise in the graphical profile.

After the surface preparation is finished the indentation site has to be identified and mapped. To do this a microindenter is used (Vickers microhardness tester). By inspecting the surface with a microscope one specific grain is chosen for indentation. This grain is then microindented along the grain boundary to easily identify the specific grain during nanoindentation as seen in figure 16. This approach is only used for the Fe3%Si samples which have been heat-treated to increase the size of the grains.

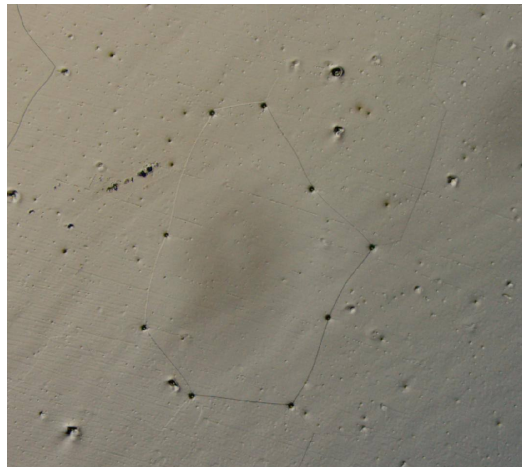

Figure 16: Mapping of specific grain on sample

4 Experimental Procedure and Results

This chapter describes the tests performed during the scope of this master thesis. The first tests are described in more detail to give good insight into the procedures. In addition, several changes which are made on the basis of each test are discussed to avoid future projects making the same mistakes and to enhance the changes which have great influence. Each test includes results, discussion and conclusion, creating the basis for each new test and the final conclusion. Since no similar experiments have been executed in any publications found the results are not directly compared to others, but discussed on the basis of permeation experiments and other in situ nanoindenation experiments. It must be emphasized that the main task will mainly be to see if it is possible to measure any effect of hydrogen with this approach.

4.1 Test 1: Identify Setup and Procedure Issues

The first experiment performed for this thesis had the purpose of testing the Fe 3%Si sample and the electrochemical hydrogen permeation cell. Based on this, possible improvements needed for the setup or procedure could be identified and the results could be used as a basis for further testing. This experiment is explained in more detail than the later experiments and includes descriptions of for instance calibration and specific nanoindentation preparation which will not be repeated.

In order to start the experiment the sample had to be mounted inside the electrochemical cell. All the different components were washed with ethanol and warm distilled water before carefully putting them together to avoid any damage to the sample. The indenter was then calibrated using a simple aluminum sample and the tip to optic calibration option. Thereafter a safety area was defined, ensuring safe navigation when the cell was installed. After calibrating the indenter on the aluminum sample the permeation cell including the Fe 3%Si sample could be fixed inside the nanoindenter. This step revealed the first issue with the cell. The stage for the cell, created to fit inside the indenter had holes which were approximately 2mm of point. This caused the stage to only be fixed properly with two screws, and loosely fixed with the other two. This could cause the cell to move, and make it difficult to locate the indents after indentation. Especially if the cell where to be taken out of the indenter for horizontal charging and installed back in. In addition to this, the misalignment also complicates the installation process.

After fixing the cell the procedure of the indentation in air could be initiated. This included defining the desired grain area for indentation using the optics and navigating by the micro indents made by the Vicker's hardness test machine. By choosing an area inside the grain, the tip

approached and engaged the sample surface, scanning the surface before indentation. The indentation was first carried out at a load of 2000uN which gave an elastic curve without pop-in. After two indents the indentation was stopped and the force was increased to 5000uN. At this load the sample displayed a pop-in load of 2500uN. Three indentation areas of 20x20um were used with nine indents in each area. Each indent was 5um away from the others and each area was 10um away from each other.

The indentations in air created the basis for comparison and electrochemical hydrogen charging could be initiated. For this procedure the cell was unfixed from the indentation stage and moved outside the chamber in a horizontal position. The cell was then connected to the electrical connections for the counter, reference and working electrode before filling the cell chamber with electrolyte. The potentiostat was set to -1500mV and the current was monitored through ECM WIN software. The sample was charged for approximately 2.5 hours before the sample was again fixed in the indenter and indented in one area.

After this indentation the cell was taken out again for new charging, this time at -1600mV and -1700mV for 5hours. The indentation procedure was then executed again in two areas before increasing the potential to 2000mV for 30min while still in vertical position inside the indenter. This was done to try and push more hydrogen trough the sample to see if there was any change in pop-in load. One area was indented while charging at -2000mV. All the results from the indentation and charging were saved on the computer before the cell was taken back out again for overnight charging. The potential was decreased to -1500mV and the cell was monitored through ”Teamview” and a camera to ensure the current was in the desired range. After the overnight charging a new indentation process was set up. This charging and indentation process was repeated three additional times, at 48, 68 and 145 hours.

4.1.1 Results

The charging current density vs time is shown for the entire experiment in figure 17. The charging intervals have been sorted by the use of color and are gathered in one single graph for overview. For a more detailed view figure 18 is added. This graph shows the typical behavior during horizontal charging, where the current is gradually decreasing before a big increase is measured and then it resumes its gradual decrease.

Indentation before charging referred to as ”indentations in air” shows the pop-in loads for the sample without hydrogen present. This is indicated in red throughout the graphs for this experiment. The indentation after 2.5 (blue) and 7.5 hours (green) of charging together with the indentation

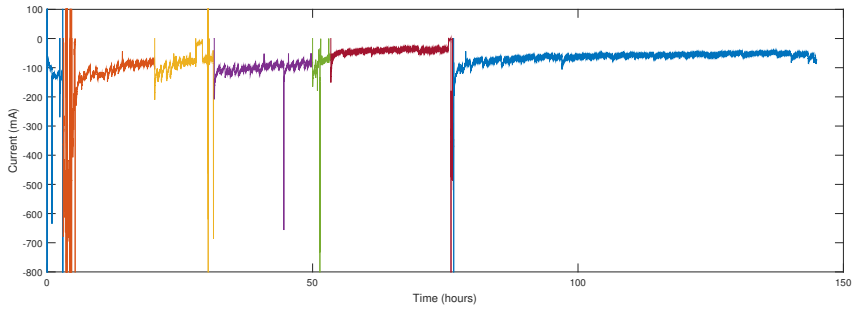

Figure 17: Charging data for all 145 hours combined

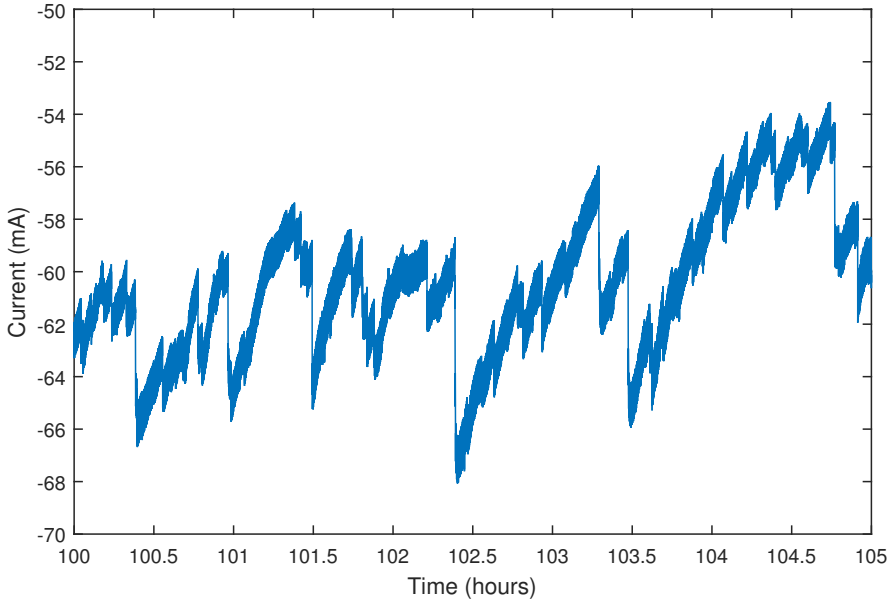

Figure 18: Detailed view of charging data from 100 to 105 hours

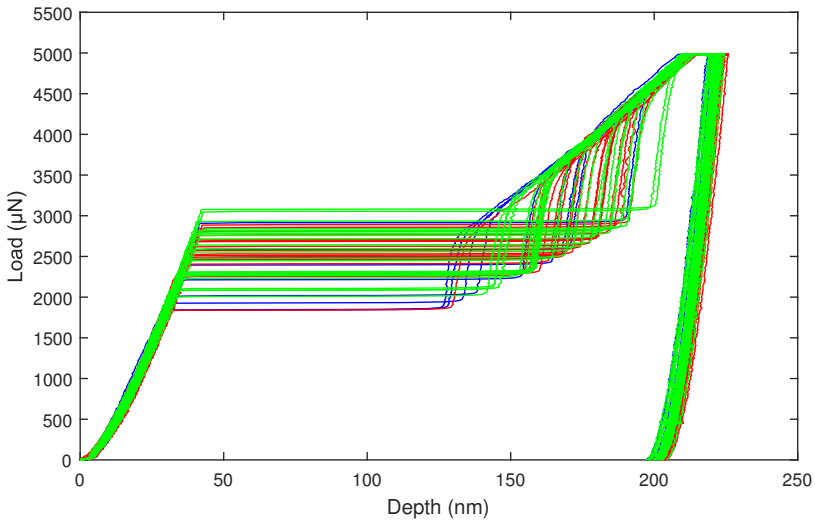

Figure 19: Indentations in air (red), after 2.5 hours of charging (blue) and 5.5 hours of charging (green)

in air is shown in figure 19. No big change in pop-in load is identified. The concentration of hydrogen at this time is uncertain.

Indentation on sample surface after 24hours of charging compared to the indentations in air in figure 20 and show a big change in material behavior. The pop-in is non-existing for the first 18 indentations (blue) in two separate areas. When the indenter is moved to the same area as the air-indents, the pop-in is back around 2000μN (green). The indenter is then moved back to the area of the first 18 indent and pop-in occur (magenta). The concentration of hydrogen in the subsurface where the indentations are made is still unknown.

The last indentations after 48, 68 and 145 hours of charging are added in figure 21. These indentations show no effect of the hydrogen.

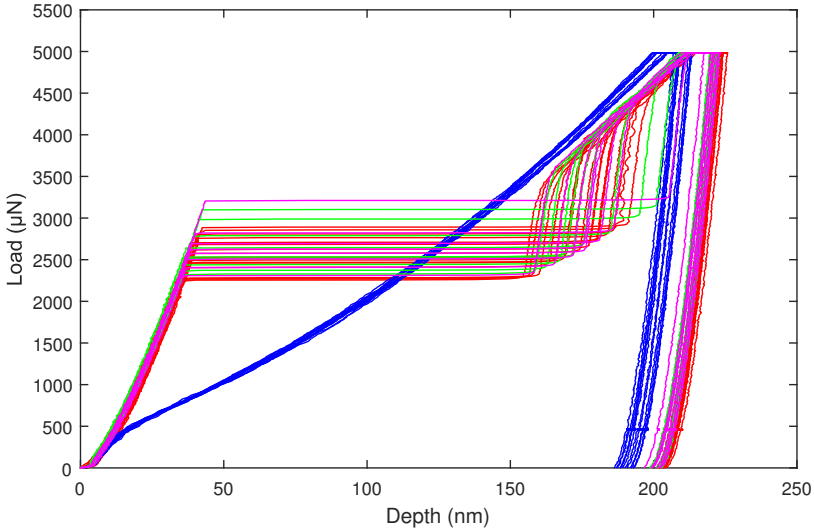

Figure 20: Indentation in air (red) compared to the two first indentation areas after 24 hours of charging (blue), one indentation area next to the indents in air (green) and one indentation area back where no pop-in occurred (magenta).

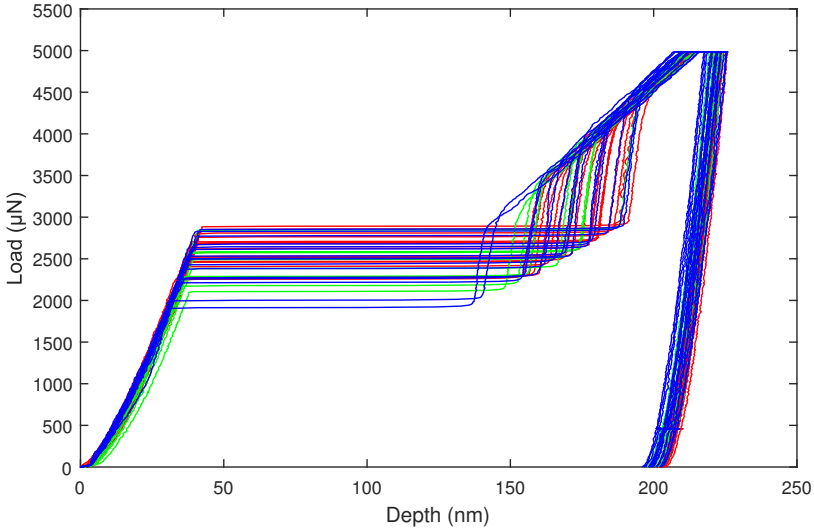

Figure 21: Indentation in air (red) compared to indentations after 48 (green) and 68 hours (blue) of charging. No change in pop-in load

4.1.2 Discussion and Conclusion

The charging which was, as seen in figure 17, not constant for the entire process can be described on the basis of several different factors. The decrease in negative current can be due to the hydrogen evolution causing hydrogen bubbles to form on the surface, hindering the flow of current. As a measure to counter this, a syringe with electrolyte connected to the inlet hole is used to inject new electrolyte into the cell, causing flow and thereby pushing the hydrogen bubbles away from the surface and out through the outlet hole. The jumps in current are usually due to this, or due to large bubbles removing themselves from the surface due to the nature of hydrogen which travels up through the electrolyte to the outlet hole. The injection is at this time done manually, but a syringe pump will perform this process in further experiments.

The big change in pop-in load after 24 hour, while no effect after 7.5 hour charging can be an indication of the effect hydrogen has on material behavior in Fe3%Si if the hydrogen is given time to diffuse through the sample. However, the difficulty in reproducing the results after the three day long charging makes it challenging to conclude with this effect.

The material used in this experiment has a BCC structure. Based on the relation between structure and diffusion rate presented in the theory it is possible that the hydrogen is not staying trapped inside the material structure for long enough or at a high enough concentration in order for the hydrogen to actually have an effect on the results. It can be that the time spent installing the cell inside the indenter, causing the charging current to drop, causes enough hydrogen to escape the sample surface before indentation is performed, making it impossible to measure any effect of the hydrogen. During the indentation process the indenter sometimes also had difficulty approaching the sample surface, causing the time from installation to indentation to increase. This problem with approaching and engaging may be connected to the installation problems with the cell stage, causing the vertical sample position to move between each approach after charging. Since there is no method to measure the concentration of hydrogen on the subsurface one cannot, based on this experiment alone, say much about hydrogen effect or how much time the hydrogen needs to escape from the subsurface into the free air.

Based on these remarks it is evident that the cell stage holes needs to be adjusted for safe and easy installation in the indenter. This should contribute to eliminate the problems with approaching the sample, thereby decreasing the time spent from installation to indentation. In addition to this the sample used for indentation should be evaluated. Three possible options is to 1) Decrease the thickness of the sample to increase the concentration of hydrogen in the subsurface. Suggested thickness is 250-400μm. This can be achieved by electropolishing the sample for about one hour

in one specific spot. Another approach would be to 2) use a material with a lower diffusion rate such as SDSS and 316 Steel, or other materials which naturally creates an oxide layer. With a lower diffusion rate, the time spent from installation to indentation is not as sensitive and the oxide layer can reduce the recombination rate as described in the theory. Using materials with lower diffusio rate will require a thin sample, since the charging time to ensure full permeation will increase compared to Fe3%Si. For some of these materials the pop-in load might not be as present and the change in hardness will have to be the measure of change. In addition to this 3) a silicone oil can be used to cover the indentation sample surface to presumably ”force” the hydrogen to stay in the sample subsurface and stall the recombination rate long enough for the indentation to measure a possible effect.

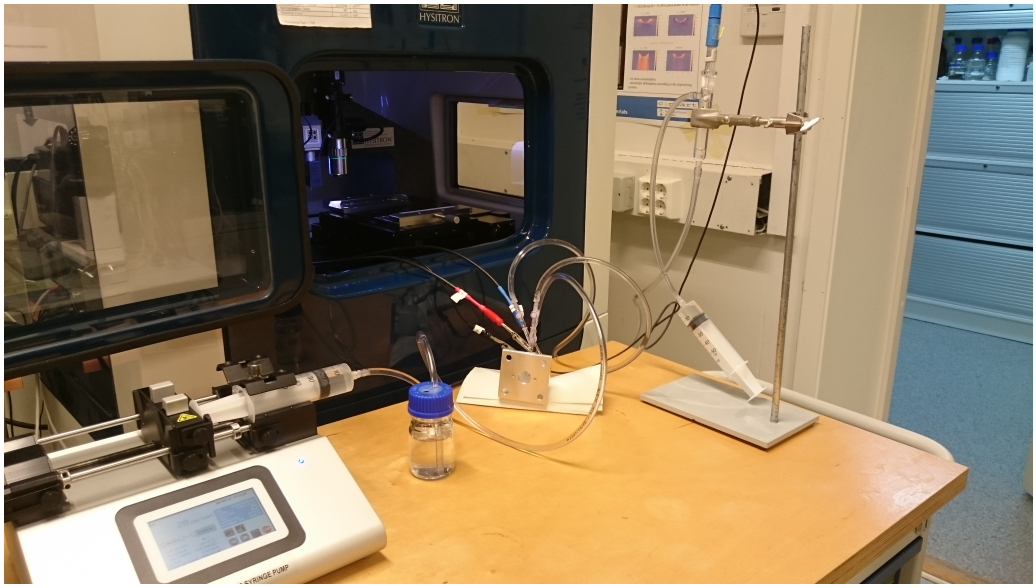

Figure 22: Complete setup of cell and syringe pump venting system

4.2 Test 2: Syringe Pump

Test two included use of the LEGATO™ 270 syringe pump. This is a dual syringe, programmable touch, continuous flow, push-pull pump which replaced the previously manual flow injections. The cell was set up as in test 1, with a 1mm thick Fe3%Si sample and the manual syringes where replaced with syringes connected to the pump. The pump was firstly put up with two syringes connected to the hydrogen outlet hole close to the sample and the outlet next to the reference electrode. Between one of the syringes and the cell a venting system consisting of a container of electrolyte which each tube went through for easy air-bubble removal was placed. Unfortunately this venting system resulted in draining of the cell during withdrawing of the syringe furthest from the venting system. To tackle this problem one of the syringes where removed and the venting was put in its place. The injection rate was set to 128ml/min and withdraw rate was set to 20ml/min. This rate was based on the observation of the effect a big push had on the current and the sensitivity for draining the cell at high pull rate. Figure 11 shows the setup with the syringe pump and figure 22 shows the complete setup with the syringe pump and the cell.

4.2.1 Result

The system was tested in both vertical and horizontal position. With a horizontal position it varied between -300uA and -800uA. As the cell was flipped in a vertical position the current quickly decreased to -200uA. Over a 4 hour (hour 7-11) period of vertical charging the current started to stabilize around -160uA. Since it was going to charge over night the cell was then flipped back into horizontal position where it started of at-600uA and steadily decreased to -300uA where it was kept relatively stable.

After the overnight charging the cell was, again, put in a vertical position for close monitoring of the current drop. The start off current for the vertical charging was -300uA. The first hour gave out a minimum current of -80uA at the end of withdrawal, and a recovery current of 230uA at the end of an injection. By leaving the cell charging for several hours the tendency of a stable lower and upper current was observed.

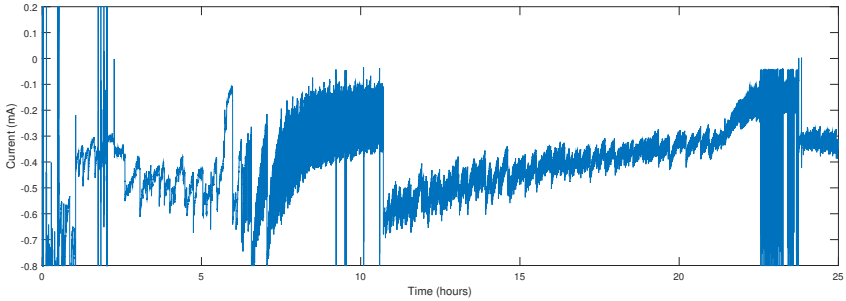

Figure 23: Charging Current in permeation cell over 25 hours

4.2.2 Discussion and Conclusion

The use of a syringe pump to replace the manually push and thereby flow of electrolyte inside the cell was without a doubt a success. However, the effect of flow on it's own is disputable as a good way of removing hydrogen on the sample surface. Although the flow of electrolyte for the most part had a visually detectable impact on the bubbles on the surface, the current vs time plot 23 combined with visual observations on the surface indicate that the flow on its own seems to have an effect on the current directly. The current increases abruptly as the injection starts but drops quickly as the withdraw process is started. This happened when bubbles were clearly removed, but also when they were not. The increase in current was usually biggest when big bubbles were removed. The current keeps dropping as the withdrawing process is in motion. How much this

effect the diffusion process is unknown, although it is known that current density is an important factor in permeation experiments[5]. Based on these results the use of the syringe pump will continue in further experiments. A possible change could be the electrolyte mixture. A more aqueous electrolyte would flow more easily in the cell, causing less pressure build-up inside the chamber, and thereby on the tube-connections. If this will result in a more stable current will have to be tested.

4.3 Test 3: Silicon Effect

For the Fe 3% Si sample, the diffusion rate is expected to be high based on the crystal structure. How quickly the hydrogen is escaping the subsurface which is reached through nanoindentation and recombining in the free air is hard to determine and therefore opens for the question if it is the hydrogen which is influencing the nanoindentation results for the experiment or not. Different possible solutions to reduce the recombination, and thereby forcing the hydrogen to stay inside the subsurface during the experiment is proposed in Test 1. For this test the effect of silicone oil and silicone grease in indentations will be tested.

4.3.1 Silicone Grease

A thin layer of silicone grease is proposed as a solution. Silicone is an inert polymer, and by mixing silicone oil with a thickener silicone grease is created. In order to test the proposal a thin layer of Silicone Grease was applied by hand on a Microscope Slide of approximated thickness 1mm. Indentation of the glass is performed first, before indentation through the silicone grease, results from this and the indentation on clean glass after indentation in silicone can be found in figure 24. The graph shows the same loading curve before and after indenting in grease, indicated by the red and blue curves respectively. The indentation process in silicone is repeated with varying set point for the tip engaging and a load of 5000μN. First the set point is varied between 20-70μN in order to obtain a proper scan of the covered surface. The results from this can be seen in figure 25 and is indicated by the green curves. The graph clearly shows that the indent is not reaching the surface and the grease is creating a resistance to disengaging of the indenter tip. Figure 25 also illustrates a different approach where the indenter tip approaches the surface with a high set point of 400-500μN, before the tip disengages 1μm and then engages again at 20μN for scanning and indentation. This is indicated by the magenta curves. Also here the grease is greatly influencing the unloading of the indenter. The change in indentation depth after the drop in loading has yet to be understood and the use of silicone grease was discarded.

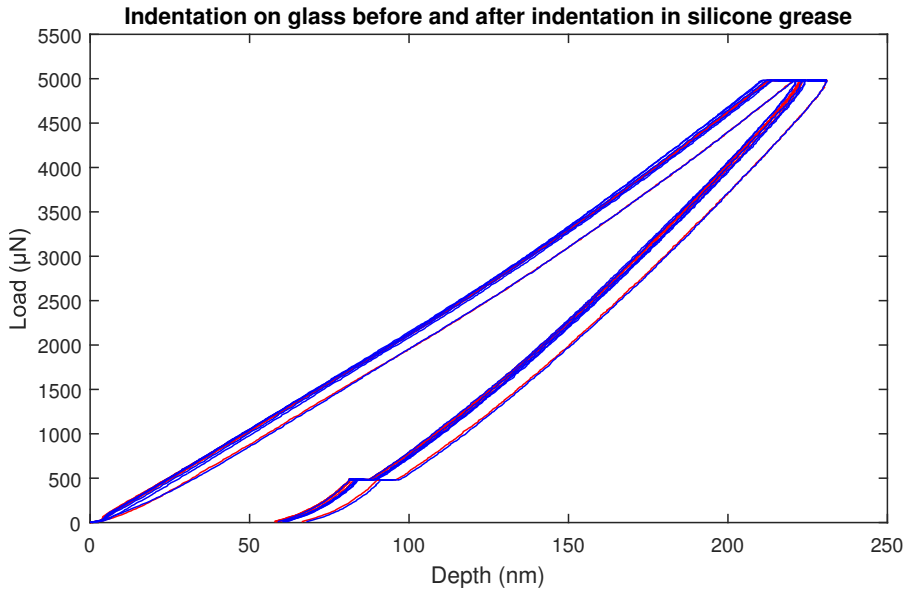

Figure 24: Indentation on clean glass surface, before and after being in silicone grease

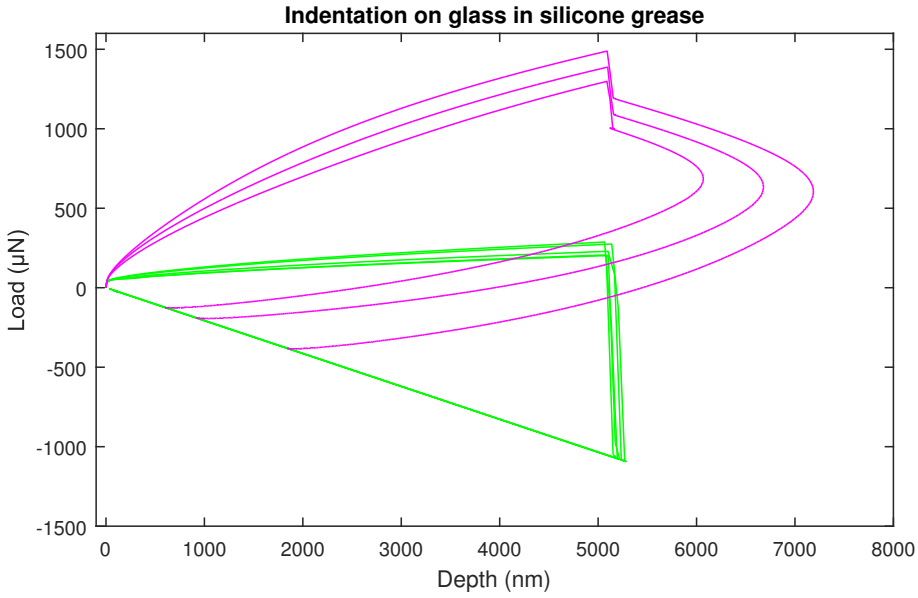

Figure 25: Indentation on glass in silicone grease with green: set point 20-70μN and magenta: set point 400-500μN

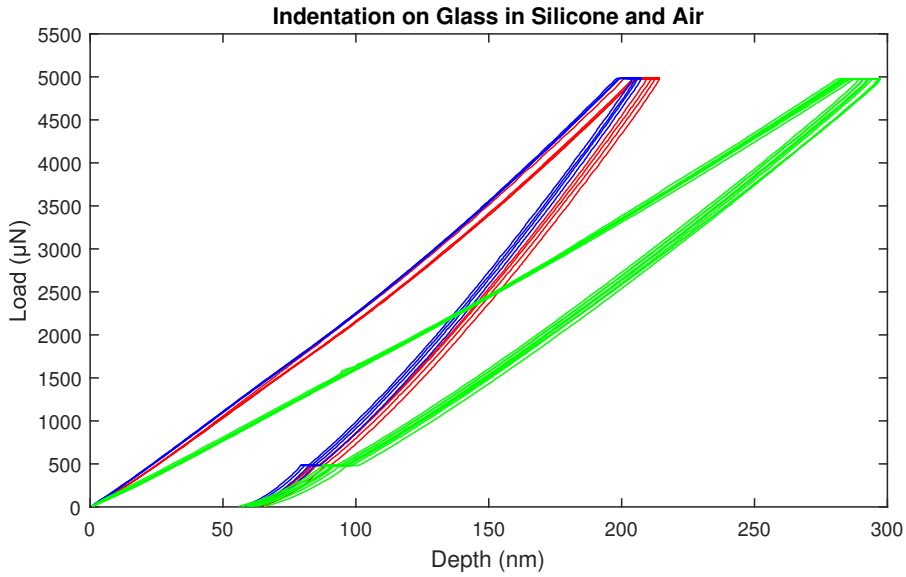

Figure 26: Indentation on glass with and without silicone oil

4.3.2 Silicone Oil

The intent by using silicone oil is to both to reduce the recombination rate as well as give an indication of hydrogen presence at the surface. To test if the oil had any influence on the indentation data a silicone oil of low viscosity (20cSt at 25°C) was put on the glass sample surface using a pipette. The same indentation procedure as for the silicone grease was conducted, but without raising the setpoint (probe engaging force) above 20μN. Figure 26 shows how the indentation on the clean sample surface before indenting in the oil indicated by the red color, the blue color is the results from indentation on clean surface after indenting in oil and the green curves describes the indentations inside the oil.

The increase in depth ($\sim$100nm) for the indentations in silicone oil can indicate that the indenter probe is indenting more easily through the glass surface due to a reduction in friction caused by the oil. This is however difficult to conclude with, and an indentation test on a metal sample is necessary to see if the behavior is the same for metals. For this a Fe 3% Si sample is used. The results shown in figure 27 display no change in the indentation curve for indentation through the silicone oil (blue curves) compared to air (red curves). Based on these results the silicone oil has no effect on the indentation results, but it does require a slightly higher set point in order to do a scan of the area after indentation.

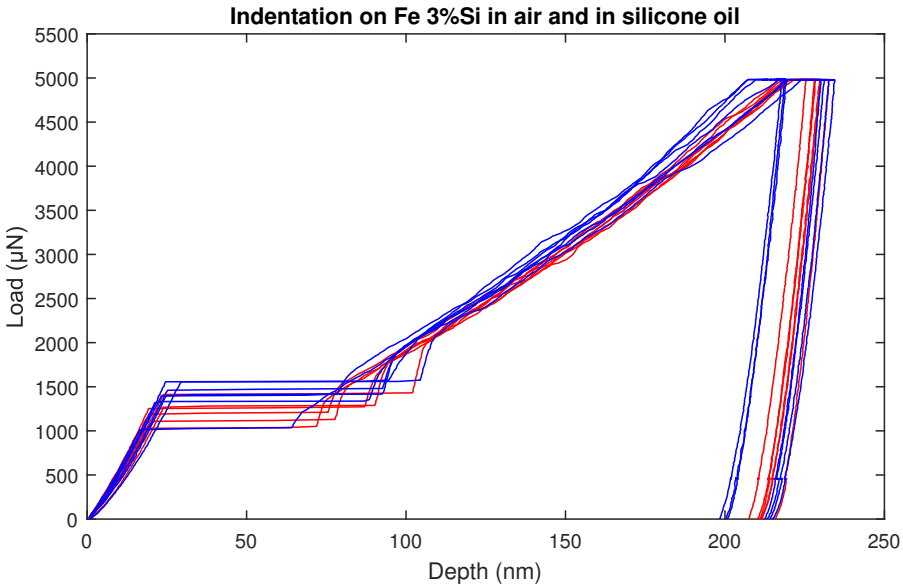

Figure 27: Indentation on a Fe 3%Si sample in air (red) and in silicone oil (blue)

Since the intent of using the silicon oil is to detect and retain the hydrogen, an electrochemical charging of the sample is necessary to see if the hydrogen can be visually detected in the oil. This is further explained in test 4.

4.4 Test 4: Silicone Oil and Thin Sample

The EHPC was setup with the syringe pump and the 400μm thick Fe 3 %Si sample used in test 3, which had been freshly electropolished with a newly made electrolyte. The electrolyte used in the EHPC was a mix of glyserin and borax with 50% water, a more aqueous solution as discussed in test 2 of the syringe pump. The charging time was set to 14 hours before the cell was put in vertical position and silicone oil was added to the indentation surface of the sample. The sample was left in vertical position and charged for 2 hours to allow for visual inspection of possible hydrogen bubbles in the oil. The sample was indented before charging, on a clean surface, and after charging, on the silicone oil covered surface. The in situ nanoindentation setup can be seen in 29. To ensure only the effect of hydrogen was measured and not the effect of silicone oil the sample was also discharged by removing the electrolyte and potentiostat and indented again in the silicone oil. The silicone oil which had a viscosity of 20cSt leaked through the seal between the sample and the top plate of the cell. The oil had to be refilled in order to maintain the covered surface.

4.4.1 Result

The charging current for the whole process is presented in Appendix A, figure 52. The indentation results presented in figure 28 illustrates the indentations before charging and adding the silicon oil as well. This is indicated by the red color. The indentations after 16 hours of charging is indicated by the blue color, which includes 14 hours of horizontal charging, followed by the application of the silicon oil and vertical charging for two hours. The indentations, after stopping the charging for two hours is indicated by the green color.

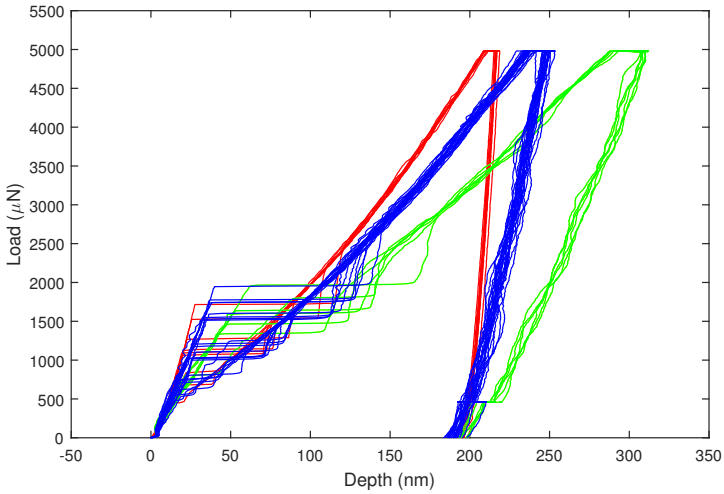

Figure 28: Indentations in air (red), after 16 hours of charging (blue) and 2 hours after stopping the charging charging (green)

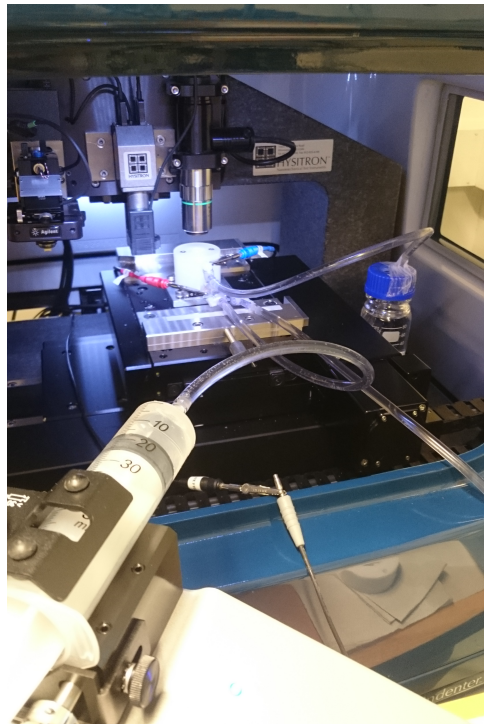

Figure 29: In situ nanoindentation setup

4.4.2 Discussion and Conclusion

The tubes for this setup was a bit short, so the venting container had to be put into the chamber, and the door to the chamber had to be kept completely open. For future experiments, these tubes will be made longer to reduce noise inside the nanoindentation chamber. The results from the experiment, illustrated in figure 28 show a clear change in the indentations curves, which could be an indication of hydrogen effect, however, there was no visible hydrogen bubbles in the silicon oil which could be seen with the naked eye. The indentation curves shift to the right for the hydrogen charging, but it does not return to its original state after the charging was stopped. This could be due to the hydrogen not being fully removed from the metal lattice and thereby still affecting the sample. However, since the first test of silicon oil on the FeSi sample was performed right after the silicon oil was applied, the long term effect on the surface is still unknown, and can thereby not be eliminated at this stage as a cause of change. To be certain that it is not a long time effect of the silicon oil, a new indentation test of the sample with silicon oil should be performed, with longer exposure time. If this test shows a change in the indentation results, one cannot conclude with any hydrogen effect, but it would give insight into the use of silicon oil during nanoindentation which could be valuable for further research. If however the results still don't change, it would mean the change could be caused by the hydrogen and further testing with this setup should be carried out.

4.5 Test 5: Effect of Long Time Exposure to Silicon Oil

Based on the results found in test 4, the effect of silicon oil on the metal surface over time had to be investigated. To do this, three samples made of namely Fe %3Si, Super Duplex Stainless Steel (SDSS) and 316 Steel were tested. Each sample was electro-polished and put inside the nanoindenter. To create a basis for comparison the samples were first indented on a clean surface. For the SDSS which consist of ferrite and austenite, several indentation where made to ensure both phases were covered. After this step, the samples were covered by two drops of silicon oil. This amount was enough to cover the whole surface, but small enough to limit spilling inside the indenter. The samples were indented straight after the oil was added, then again after 2-3hours and one last time after 20 hours.

4.5.1 Results

Surface scans of the surface after indentation is shown for all three different materials in figure 30. The indentation results on the next page illustrates the indentations before silicon oil is added (red), indentations after applying the silicon oil (blue), indentations after 2-3hours of silicon oil coverage (green) and indentation after 20-21hours of silicon oil coverage (magenta) for all three materials. The samples were indented in the order in which they are presented; 316 Steel, SDSS and Fe3%Si respectively.

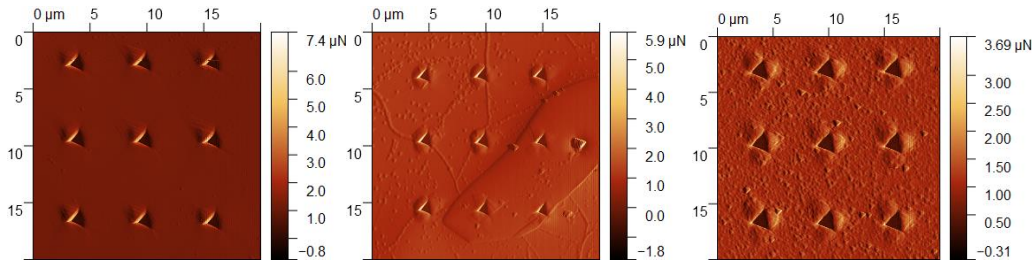

(a) 316 Steel **(b)** SDSS **(c)** FeSi

Figure 30: Surface of material after indentation

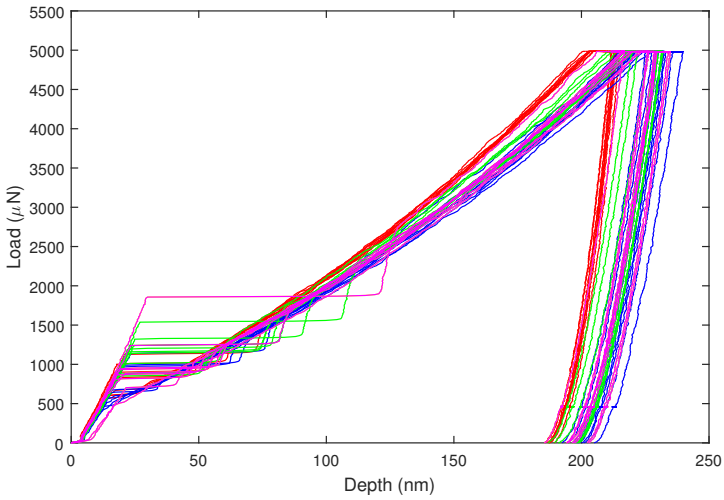

Figure 31: Change in indentation results on 316 Steel sample for long time coverage of silicon oil

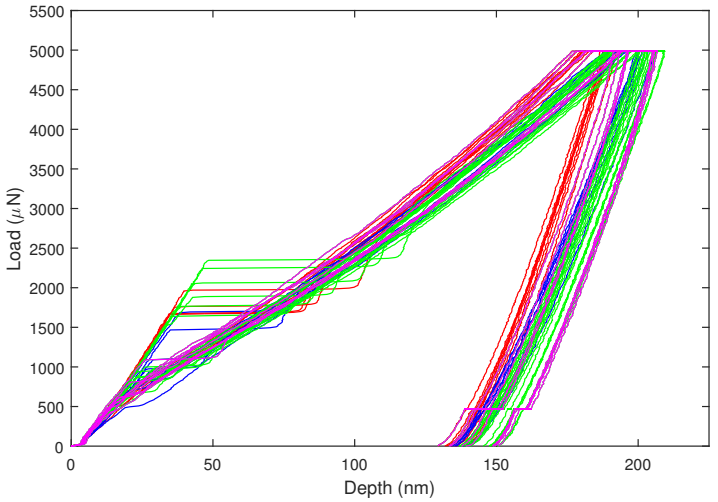

Figure 32: Change in indentation results on Super Duplex Stainless Steel sample for long time coverage of silicon oil

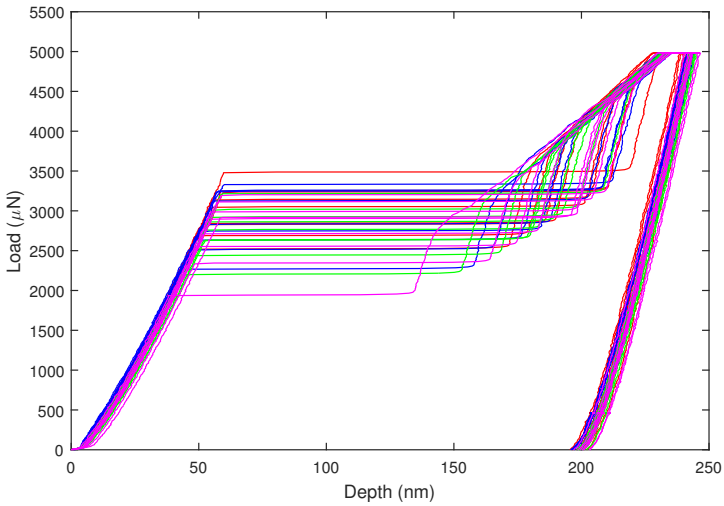

Figure 33: Change in indentation results on Fe3%Si sample for long time coverage of silicon oil

4.5.2 Discussion and Conclusion

For the SDSS and 316 Steel the samples show a slight change in the indentation curve for the Silicon covered surface. However the time of coverage seem to have little effect on the overall effect. Since both SDSS and 316 Steel include austenite, the un-magnetic allotrope of iron, it could mean that it is this phase which is mostly influenced by the silicon oil. This is however impossible to conclude with based on this simple test. For these two materials, the use of silicon oil for indentation should therefore be done with caution, and the effect should be included in the overall interpretation of the indentation data.

For the Fe3%Si sample on the other hand, the change is non-existent, even over time. This correlates to the previous tests for short time coverage and supports the theory which claims that the change in indentation results obtained from test 4 were actually due to the hydrogen effect. Based on this, more test with the setup from test 4, including the silicone oil should be performed to investigate if the results are reproducible and could contribute to understanding the hydrogen effect.

4.6 Test 6: Silicon Oil and New Counter/Working Electrode

Based on test 4 and 5, the need for a second experiment with the same setup is required to check if the results are reproducible. For this experiment the arrival of the custom made counter electrode, made from platinised titanium, together with a new working electrode, this time in cobber instead of aluminum does create small changes in the setup. Despite this, it is not expected to influence the result and should make the setup safer for use inside the nanoindenter. The EHPC was setup similar to test 4, with the mentioned changes. The silicone oil was added right away and indentations were made. It took 7 different indentation areas to find one which had pop-ins and stable curves. 18 indents were made in this area before charging was started The cell was then left for charging in horizontal position for 23,5 hours before the cell was flipped into vertical position for 1hour. When the cell was flipped it was discovered that the seal between the top plate and the sample had fractured. This caused the silicone oil to leak. Despite this, indentations were made on the grain in the designated area. This was very close to the fractured seal, which led to contact with the seal when trying to withdraw from the sample. Based on this it was decided to try and remove the seal and tighten the cell again, similar to test 5. As the seal was removed, the cell started to leak. Unable to fix this leak, caused electrolyte to cover the top surface of the sample as well, and it was decided to abort the test.

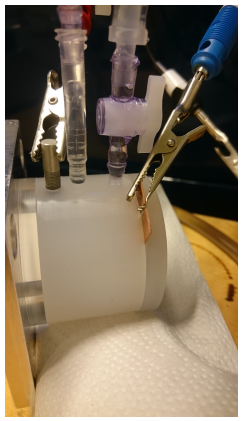

(a) New counter electrode to the left and new working electrode to the right

(b) View of counter electrode inside the cell during charging

4.6.1 Results

Charging data from this test can be found in Appendix A, figure 53. The results from indentation before charging inside the silicone oil is indicated in blue and green in figure 35. The blue plots

are from the first 6 indentation areas. The green plots are the 18 indentations done at area 7. This figure shows all the indentations which had to be performed in the process of finding an indentation area which gave proper pop-in values and steady nice plots. To show how much the pop-in values can vary inside one grain a 3-D discrete sequence data plot is given in figure 36, where the indentations are positioned similar to the actual indentations sites based on coordinates and the measured mean pop-in load at each location is given and marked with a data cursor.

To compare the indentations before and after charging figure 37 is added. Here, the indentations before charging are still in green color and the indentations after charging is indicated in red.

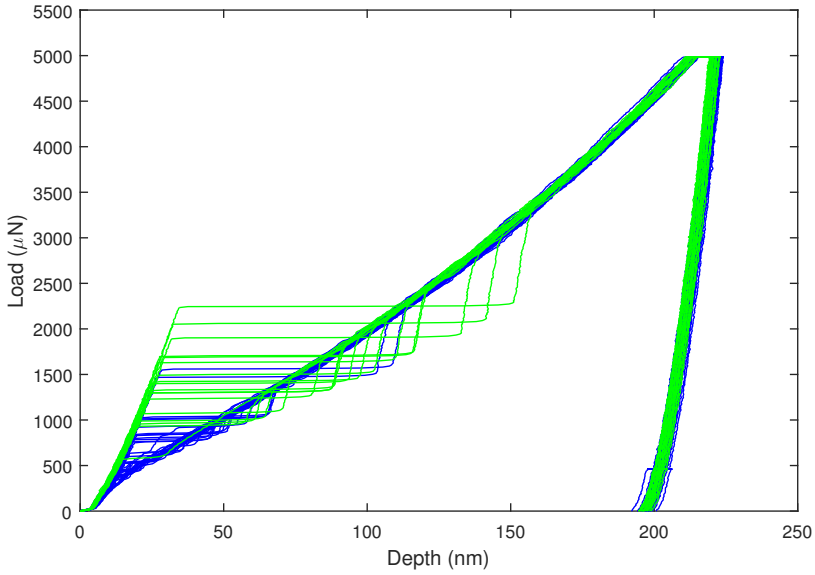

Figure 35: Indentations before charging, the green indentations are in the chosen area for further indentations

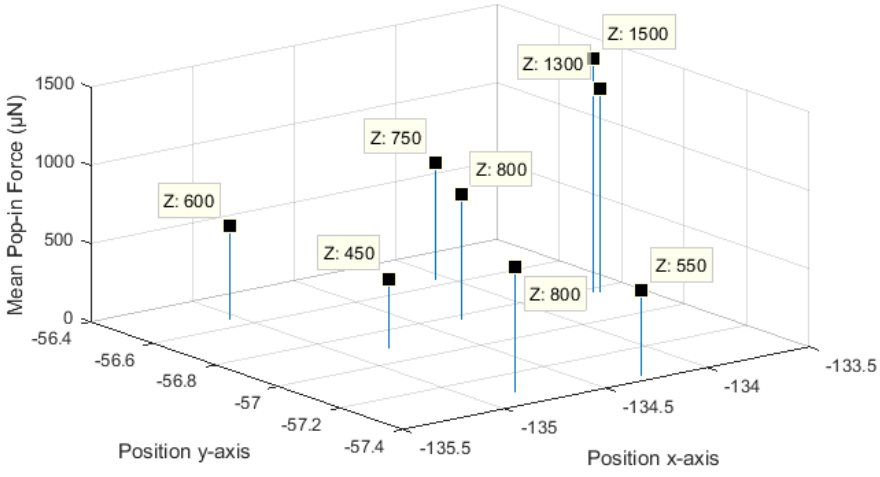

Figure 36: Mean pop-in values at the different indentation sites inside the grain

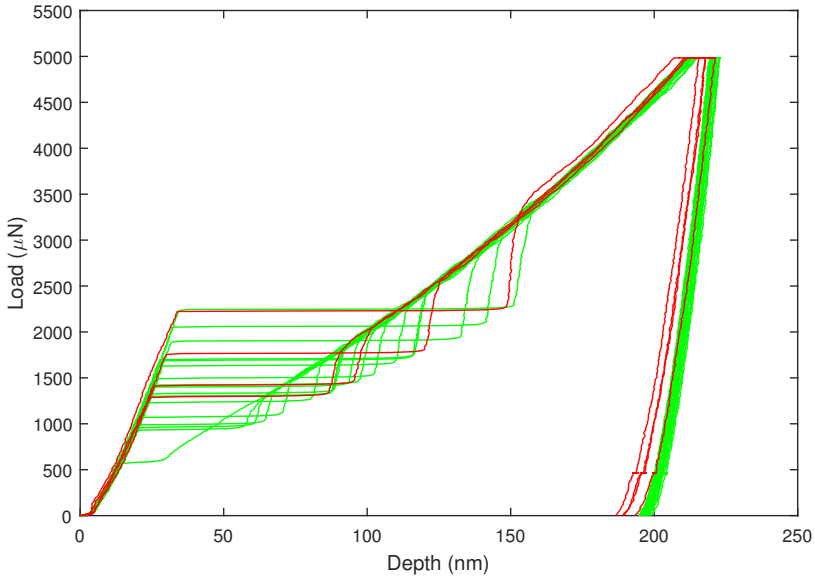

Figure 37: Indentations before indentation in green and after charging in red

4.6.2 Discussion and Conclusion

Based on the above results it is clear that which area inside one grain one chooses to indent on has a big influence on the pop-in load for this material. This can be the reason why the big change in pop-in load was found in test 1 and was not reproducible. Although pop-in was found close to the area of non-pop-in for test one, this result alone cannot be concluded as a proof of hydrogen effect. It rather gives a warning that changes in pop-in might not be a good measure of change for the Fe3%Si material when measuring hydrogen effect.

Based on the after charging results for this test, no effect of hydrogen could be seen. Even though the results are few for this test, they show no indication of effect similar to test 5.

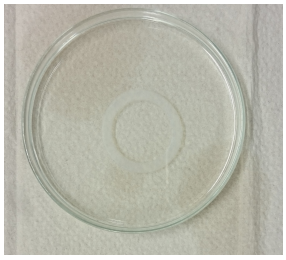

(a) Silicone Rubber Seal in Silicone Oil, 24 hours of exposure

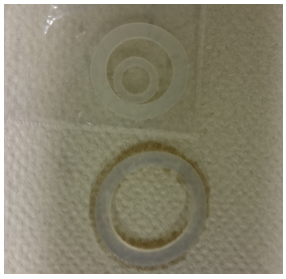

(b) Effect of exposure to silicone oil on silicone rubber seal

The seal which ruptured during the experiment was a Vinyl Menthyl Silicon Rubber. A hypothesis of why this happened is that silicone oil is absorbed by the silicone rubber, causing it to expand in size. Since there was little theory on this, a simple test was performed. A silicone rubber seal was placed in a small container and silicone oil was added covering the seal. The seal was then left over night. The observations made the day after showed a huge increase in diameter. This can be seen in figure 38a a, which shows the seal in the oil and in figure 38b b where two equal seals are placed next to each other, one which has been in the oil and one which have not. Based on this it was decided to change the seal between the top plate and the sample and perform a new test.

4.7 Test 7: Silicone Oil and Charging with Change of Seal

This test was performed the day after test 6. The sample was polished and electropolished again to avoid any contamination from the previous test. The setup was the same, but with a new seal between the top plate and the sample. For the first time the cell was left in vertical position over night (20 hours). Since the current had been observed to being relatively stable for vertical charging it seemed like a good time to try it for a long time. If this was successful, charging could be done inside the indenter, avoiding one step in the indentation process, making the setup ”more” in-situ.

4.7.1 Results

The cell showed no sign of any leakage as it was left for overnight charging however after this charging, leakage was found. The current had however been relatively stable through the night and there was still silicone oil covering the sample, so it was decided to do indentations as seen in figure 39. The flow of electrolyte created by the syringe pump was turned off to avoid too much spilling inside the indenter. The charging data from this test can be found in Appendix A, figure 54.

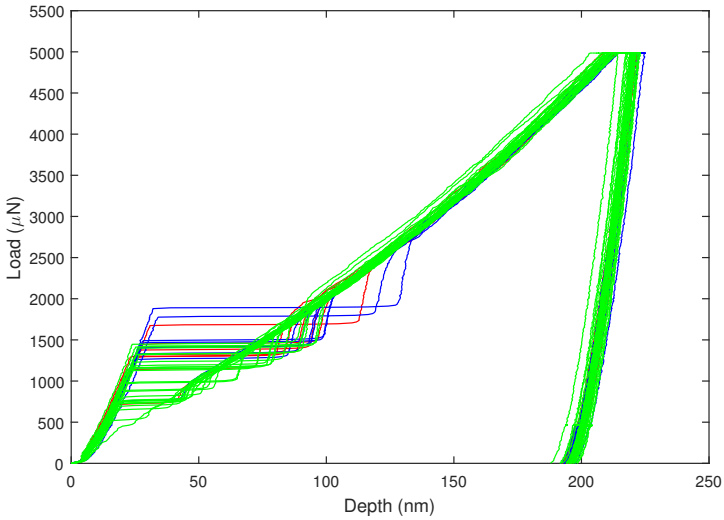

Figure 39: Red: Indentation before charging, Blue: Indentations before charging, in silicone oil, Green: Indentations after charging, in silicone oil.

4.7.2 Discussion and Conclusion

The leak in the cell seemed to be coming from the seal between the sample the main part of the cell. Since the leak did not improve after fastening the cell was not recharged after indentation. After opening the cell, it was found that the seal was a bit uneven. If this was the root cause of the leak is difficult to conclude with. No leakage like this has been observed in previous charging. Since the seals are custom made at the local workshop, small varieties can occur. For further testing it should be double checked if the seal is leveled, the sample is centered and the working electrode is not interfering with the seals.

The indentation results for this experiment show no change in any behavior, similar to test 6. The indentation process was carried out while the cell was still charging, although the current was a bit more unsteady due to the leak. Based on the thin sample and the long time charging there should be hydrogen in the subsurface if the previous results are due to hydrogen. However, since there is no practical way to know the hydrogen concentration in the subsurface with this setup concluding with one or the other is difficult. At this point one can question if it is the setup or the theory which is lacking. An analysis of the surface should be performed to evaluate is there is any corrosion on the cathodic side of the sample, hindering the hydrogen to be absorbed on the surface.

Possible changes to the setup could be adding an anodic side to the cell. This would enable a measure of hydrogen diffusion, which could give in indication if one could expect hydrogen presence in the typical charging times which have been used. Also simple calculations of the estimated hydrogen concentration at the indentation site can be performed. To do this, diffusion rate and concentration data from diffusion experiments using the same material, electrolyte and current can be used.

A similar permeation experiment was set up in 2015, the description of this wan be found elsewhere [5]. The diffusion rate and hydrogen concentrations found through this work is presented in table 2 where method one is the single anodic polarization between transients and method two is double anodic polarization between transients.

Based on equation (6) possible hydrogen concentrations at 200nm from the anodic surface is thereby given in table 3. 200nm is the total indention depth for the Fe3%Si sample in this test, but it is important to note that the pop-in is already present at 20-30nm and using this depth would reduce the concentration even further. This clearly shows how drastically the concentration drops through the sample thickness. It is however important to note that this data is not directly applicable since the conditions are not the same. The biggest difference is the fact that the cell

Table 2: Diffusion Rate and Hydrogen Concentration of permeation experiment on Fe3%Si sample [5]

Method	D_{eff} $[m^2s^-1]$	$C_0[ppmW]$
1	$3.77*10^-11$	$2.17*10^-2$
1	$3.98*10^-11$	$1.75*10^-2$
1	$4.14*10^-11$	$1.58*10^-2$
2	$3.5*10^-10$	$1.41*10^-2$
2	$2.5*10^-10$	$1.32*10^-2$
2	-	$1.26*10^-2$

used in the tests so far, does not have any electrolyte and imposed current on the anodic side. Based on this, the assumption of zero concentration on the anodic surface is not correct and this can be assumed to be higher. Also the diffusion for the referenced experiment was found to be controlled by the surface due to formation of oxide layer and carbon contamination on both sides. Pitting and etching was found on the andic and cathodic side respectively. Based on this the values which have been calculated can only be used as guidelines, rather than actual parameters for this cell, but gives a clear picture of the reduction one can expect.

Table 3: Calculated concentration at 200nm from andic surface based on table 2 for 1mm and 400μm sample

Method	Sample Thickness [μm]	Concentration C_{200nm} [ppm W]
1	1000	$4.28*10^-6$
1	400	$1.07*10^-5$
1	1000	$3.5*10^-6$
1	400	$8.75*10^-6$
1	1000	$3.16*10^-6$
1	400	$7.9*10^-6$
2	1000	$2.82*10^-6$
2	400	$7.05*10^-6$
2	1000	$2.64*10^-6$
2	400	$6.6*10^-6$
2	1000	$2.52*10^-6$
2	400	$6.3*10^-6$

4.8 Test 8: Surface Condition after Charging

Based on the lack of change in the material behavior after charging the sample surface was inspected for possible corrosion or deposition which could lead to the hydrogen not absorbing on the surface and thereby having problems diffusing through the sample. Visual inspection revealed color changes on the cathodic side and characterization of this side was performed by SEM (Scanning Electron Microscopy) and EDS (Energy Dispersive Spectroscopy) analysis. Pictures of the sample was taken with both the SEM see figure 41 and the Confocal Microscope 40.

4.8.1 Results

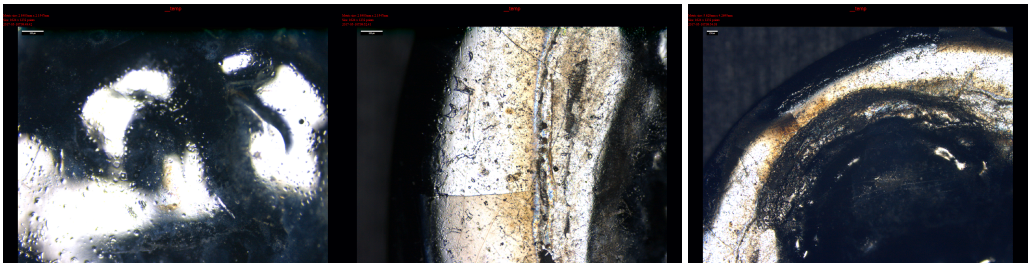

(a) Middle of sample **(b)** Outer edge of sample **(c)** Slope area

Figure 40: Surface of material presented by Confocal Microscope imaging

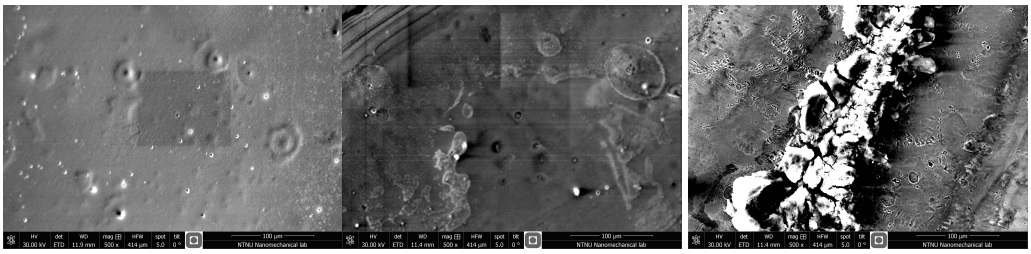

(a) Middle of sample, flat even surface **(b)** Outer edge of surface, rougher than middle **(c)** Slope area between middle and edge

Figure 41: Surface of material presented by SEM imaging

4.8.2 Discussion and Conclusion

The EDS analysis showed spots with high Cu and C content at the outer edges of the sample. It is unsure where the Cu originates, since the only contact the sample has with Cu is through

Table 4: Summary of element content at EDS spots for Fe3%Si sample after hydrogen charging

Content (Weight %)	Edge	Middle	Slope
B	1-9	1-2	0.3
C	1-24	1-3	1-2
O	1-7	0-8	30-35
F	2-9	2-4	0-0.7
Cu	0-43	0-8	0
Na	-	-	0-4
Mg	-	2-3	0-1
Si	1-4	1-4	26-35
Cr	0-2	0-1	0.3
Mn	0-1	0-1	0.1-0.3
Fe	4-90	70-95	23-42

the working electrode. It could have been transferred trough one of the leaks which have been experienced, but this does not explain why only the specific spots on the outer edges have been affected. In the areas of high Cu and C content, the content of Fe is at its lowest.

The middle of the sample has the least contamination on the sample surface. Here the Fe content is high and other contributions low. Some content remains from electrolyte, like B is found, similar to the edge part. (electropolishing and charging electrolyte). This is good for the experiment since it is in this area the indentation is performed and will therefore be the area where the hydrogen diffusion is the most important.

For the sloped area, the Si and O content was much higher than other places. This can be due to the long time electropolishing, causing the Si to build up in this area. Other contributions were low in this area. All the different areas displayed an amount of F content. This is assumed to be from the cell base material.

Based on these observation it is not evident that the surface condition should effect the hydrogen absorption and diffusion to a big degree. Especially since the area beneath the indentation area shows very little contamination. It is therefore still assumed that the hydrogen should be able to diffuse through the sample in the given time scope of charging.

4.9 Test 9: Microindentation

Given the previous tests one definite conclusion is hard to determine since the results are varying. The last tests show no change, in neither pop-in load nor hardness. It is unclear if it is the setup which is not working as well as initially assumed, or if it is the theory of measurable change due to the hydrogen at nanoscale which is lacking. In order to eliminate some of the uncertainties two different approaches have been proposed. 1) Microindentation using the Vickers micorindenter, to determine if we see any changes when the scale has been increased and the depth of penetration has a larger chance reaching a critical hydrogen concentration. 2) Full permeation experiment with anodic side in addition to the already existing cathodic side to determine if there is any hydrogen coming through the sample. This test will describe the execution of the first approach.

For the microindentation the microindenter was firstly tested for use inside the EHPC. One objective was removed to avoid crashing with the cell and a specific sequence for handling the indenter was defined. This was necessary due to the location of the sample inside the cell. The machine is designed to do indentations on a sample which is positioned to be the highest point. For the EHPC the cell is the highest point, resulting in the indenter crashing in the cell before reaching the sample surface. To avoid this, the 10x objective lens is first positioned above the sample surface. The working distance for this objective is 5.6mm, so the sample had to be put inside the groove for the seal which is 1mm deep. This gives a distance from the sample surface to the top of the cell to 5mm and gives the objective 0.6mm to travel across the cell. But it also creates the necessity for a sample which is larger than 1.5mm thickness to ensure a connection the working electrode. A 2mm thick Fe3%Si sample was therefore used. The limited working distance of the objective lens also eliminates the possibility to use a seal between the top part of the cell and the sample. Based on this the silicone oil will not be used on the sample surface for this test. The cell, fixed in the microindenter can be seen in figure 42. This shows that only one screw could fix the stage of the cell to the stage of the microindenter. To ensure a more secure fix a new stage for use inside the microindenter should be used. The design can be found in Appendix B.

After the indentation area and the best resolution is defined the specific position of the wheel controlling the z-axis is marked. By turning the wheel 6 rounds the objective lens is moved up from the sample, to a safety height. At this point it is possible to move the turret and thereby moving the indenter over the sample surface. The indenter is then lowered again by turning the z-axis wheel 6 time to the same height as the objective found the best resolution. Due to the lack of a measure of z-axis movement, the marking on the wheel was found to be the easiest and safest method to use. Only after this process is performed the actual indentation can start.

For this test the load has been set to 2kg(19.6N), the highest possible load for the machine. If the hydrogen effect is measurable with microindentation this load should definitely show it. The indentations where gathered within one specific grain to avoid any effect of grain direction. This limits the number of indentations which are possible to make and since the sample used is not heat treated the grains are now smaller than for the sample used in the nanoindentation which limits the number of indentations further.

Three indentations in different areas in the grain were made before charging. The sample was then charged for 24 hours before 2 indentations were made. 24 hours has been the general charging time for the 400μm-1mm thick samples, but since this sample is 2mm an additional 27 hours was added before the last 3 indentations were done. Unfortunately the potentiostat stopped at 50 hours due to a prefixed limit, the charging data can be found in Appendix A, figure 55. The three last indentations were therefore made one hour after charging.

To interpret the results in addition to the hardness value calculated by the machine the sample was put into the SEM for analyzing.

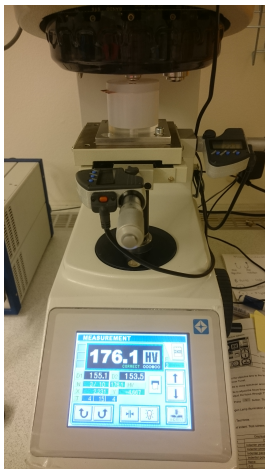

(a) Working view of the cell fixed in the microindenter

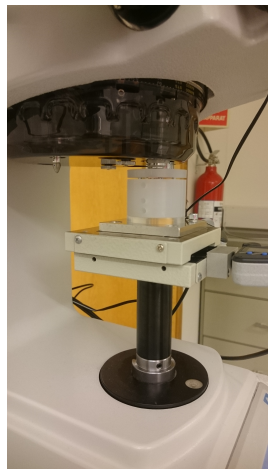

(b) Side view of the cell fixed in the microindenter

Figure 42: EHPC inside the microindenter

4.9.1 Result

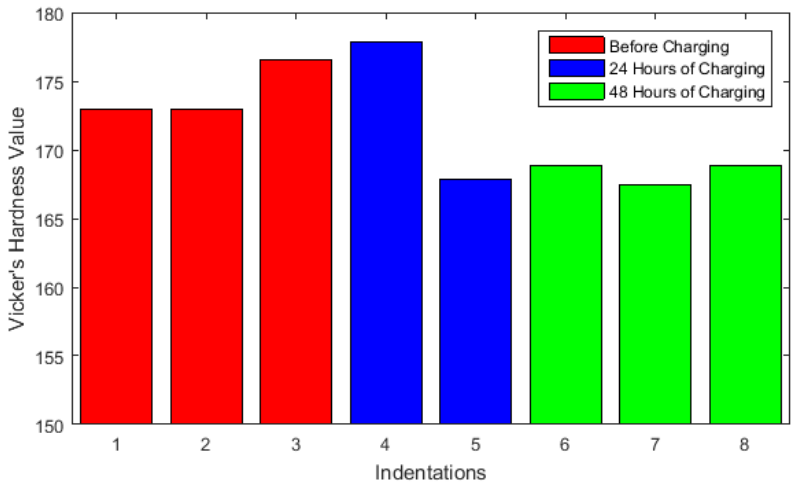

Figure 43: Hardness values for indentations

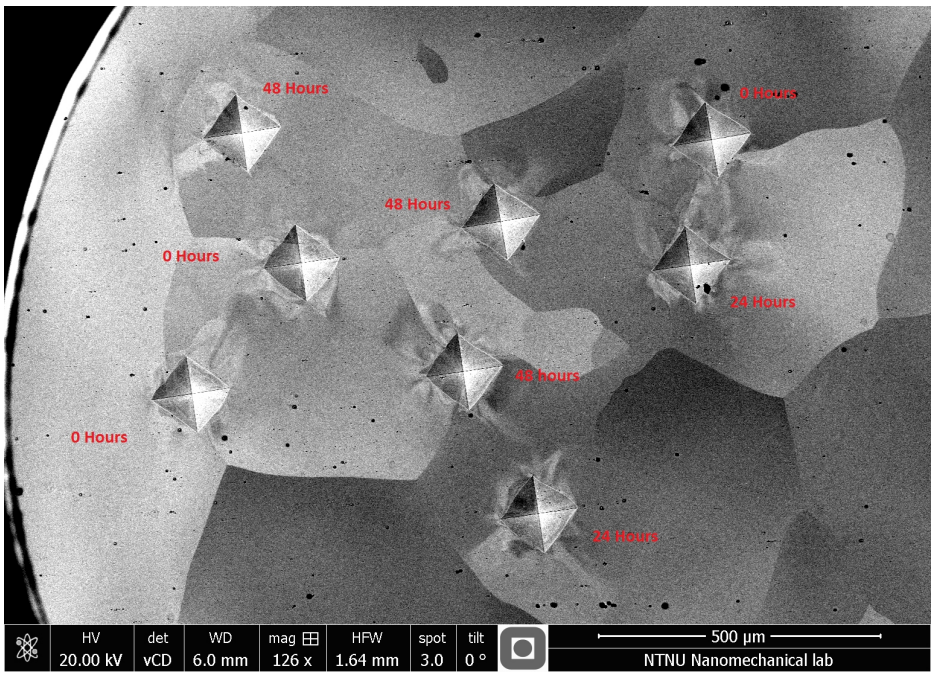

Figure 44: Overview of all microindentations

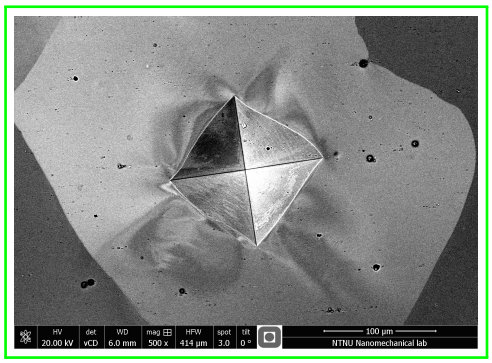

(a) Before charging

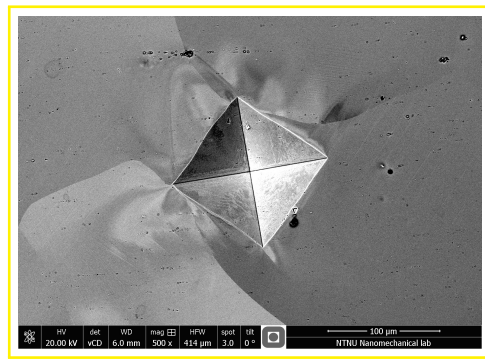

(b) 24 hours of charging

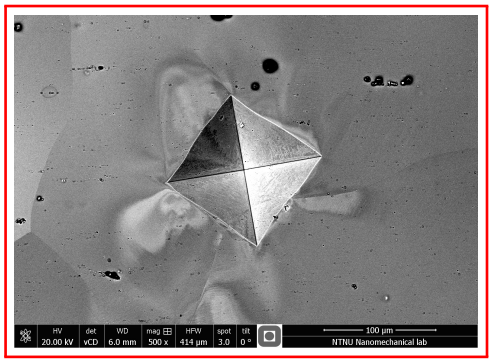

(c) 48 hours of charging and one hour without

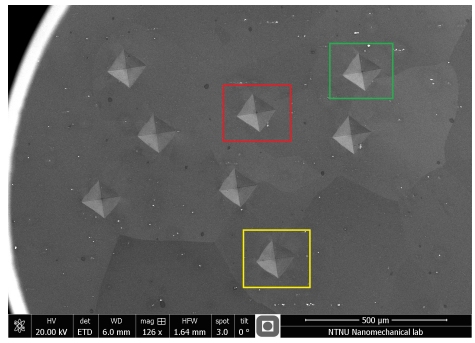

(d) Marking of detailed indentations

Figure 45: Detailed view of indentations

4.9.2 Discussion and Conclusion

Based on the result found using the SEM there is no obvious changes in the plastic zone between 0, 24 and 48 hours of charging as seen in figure 45. The indentations are located in different grains as seen in figure 44 and on some of the grain boundaries. This was first discovered during the SEM imaging, since the optical microscope could not differentiate these grains. It was however somewhat anticipated due to the lack of heat treatment causing smaller grain sizes overall. This can be the reason why the indentations under similar conditions produced different hardness values. The effect of the placement should however not be a dominating parameter for the change in hardness value due to hydrogen charging. No clear change was found between the indentations before and after hydrogen charging that could prove any hydrogen effect on material behavior. It must however be noted that the hardness values obtained using the Vicker's hardness tester shown in figure 43 is based on manual measurements, which can greatly influence the measured hardness

value. An action to reduce these errors includes the same person executing the measurements and additional inspection of the indents in the SEM after indentation.

Based on the missing hydrogen effect measured at a deeper depth raises the question if there is enough hydrogen concentration at these indentation sites to see any effect. Calculations based on previous similar work gave an estimation of the hydrogen concentration one can expect at the depths where the nanoindentations are being performed. Since the thickness of the sample was increased to do the experiment, the microindentation depth of 22.7μm calculated based on equation (9) gave concentrations 100 times the concentration of the nanoindentation. However, if this concentration in the $1-3x10^{-}4$ range is enough to measure a hydrogen effect is hard to determine. This test gave no indication of this.

In order to give this microindentation approach another try a last attempt at permeation and indentation testing can be performed. This time, on a oxide forming material with both high diffusivity and solubility to increase the probability of hydrogen being present at the indentation site. A material which has these properties is for example Palladium and Zircodium Alloy. Since we had access to a thick enough sample for microindentation in the Zircaloy-2, this was chosen for test 10.

4.10 Test 10: Microindentation on Zircaloy-2

For this test a Zircaloy-2 sample with a diameter of 12mm and a thickness of 1.9mm was used. This thickness is sufficient for use inside the microindenter. It was evaluated that the same glyserin/borax based electrolyte as used in the other test could be used for this material. However the potential would have to be set by trial and error approach. The sample was polished with 1000, 2000 and 4000 grit, followed by a 3μm and 1μm diamond polish and cleaned with ethanol and ultrasonic bath. It was then mounted inside the EHPC and an initial potential of -1500mV was imposed. This created a current in the 1-10nA scale which was too low. To find a potential producing a similar current range as for the FeSi sample the potential was varied between -1500mV and -2500mV. Through this experimental approach it was found that the potential of -1950mV produced a current in the -150μA - 300μA range which was accepted. There was however big fluctuations in the current, something that can be due to the rougher sample surface.

The sample was indented 5 times in different locations on the sample before charging. Since the sample was not electropolished the grain boundaries could not be seen in the optic microscope. The indentations were therefore indented in a pattern which enabled easy navigation for the indentations after charging. The sample was charged for 38 hours and 5 indents were made in relative close approximation to the indents in air. This was done to increase the probability of two indents, one uncharged and one charged, could be found within one grain, eliminating the effect of grain orientation.

4.10.1 Result

Charging data and measured hardness values are given below. The bar diagram of the hardness value is divided into indentation position and the hardness values before and after charging marked in blue and yellow respectively.

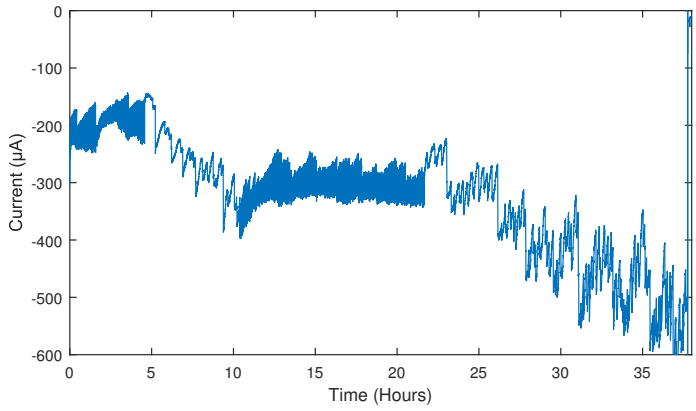

Figure 46: Current during charging for test 11

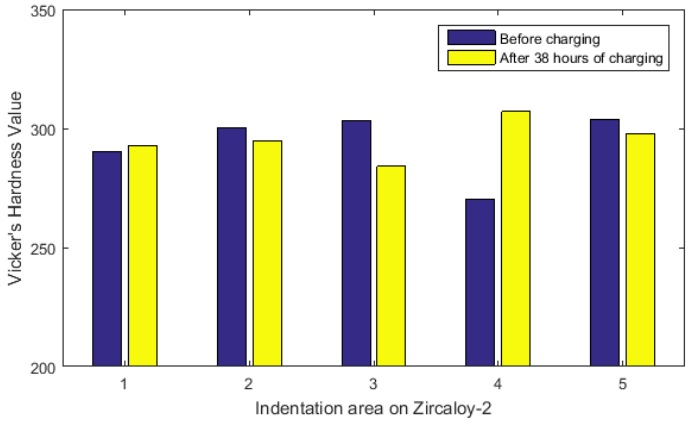

Figure 47: Measured Vicker's hardness values from test 11

4.10.2 Discussion and Conclusion

Finding a current in the same range as previous experiments turned out to be more difficult than anticipated. As the -1950mV potential was chosen for overnight charging the current fluctuated greatly and the current over time increased from -200μA to -400μA during the first 24 hours and increased further to -600μA after 38 hours. After 38 hours of charging the surface on the cathodic side was clearly affected and had a black and blue surface color. This corresponds to the oxide layer found in similar permeation experiments [31] with Zircaloy-4 where the surface oxide layer was describes as uniformly black and compact, although created by different means.

In addition to the surface condition the pump was experiencing troubles. The pump stopped after 5 hours, and since this was overnight the pump was not started again until 6 hours later. The same happened during the second night of charging after 24 hours of charging the pump stopped and was not restarted until hour 38. This can clearly be seen in the charging data where there is more noise in the data when the pump is running but the current is more stable. When the pump is turned off the current is continuously increasing negatively, thereby increasing the hydride formation on the Zircaloy-2 and could be the reason why there was such a big effect on the sample surface on the charging side.

The results from this test show a slight increase in hardness after charging for three out of five indentation sites and a decrease in two of the indentation sites. The change is however small in four out of five sites, and does not create a basis to conclude with any effect due to hydrogen. It must however be pointed out that the formation of the thick oxide layer on the sample could have reduces the hydrogen absorption and thereby the hydrogen concentration over time.

Due to the project time limit, this was decided to be the last indentation experiment. The only experiment remaining was therefore the permeation experiment with a custom made anodic top part of the cell.

4.11 Test 11: Full Permeation Experiment, New Anodic Side

The full permeation experiment was the second approach proposed in test 7. The purpose of this test was to determine if the hydrogen was diffusing through the sample in the time scope assumed through the previous tests. This would give an indication if the cell was working the way it should and could also contribute with some diffusion rate data for future work. To do this, a custom made top plate of the cell was designed and manufactured. The design can be seen in figure 48 and machine drawings are found in Appendix B. The setup can be seen in figure 49 and is similar to the initial setup for the cell but with the addition of the anodic charging side. It was decided not to use the syringe pump since it could have an influence on the current which was being monitored. The same electrolyte (glyserol, borax and distilled water) was used on both sides of the cell.

The first step in this process was to remove any hydrogen present in the sample. To do this only the anodic side was covered in electrolyte and the potential was set to 0V, the current was monitored to see when it stabilized. After approximately 2 hours the charging on the cathodic side was initiated with the potential of -1700mV, this caused a very high cathodic current. In order to avoid to much hydrogen being produced and forming on the sample the potential was decreased to -1500mV and the potential on the anodic side was kept to 0V. In addition to the charging to see if there was hydrogen passing through the sample an attempt to create a polarization curve was performed. For this curve only the cathodic side was needed. The cell could therefore be put in a horizontal position to avoid too much hydrogen forming on the sample in the absence of the pump. The potential was set to start at -2000mV, increase to +1500mV and decrease back to -2000mV within two hours. This is much faster than the standard for polarization describe but should limit the time the sample is kept at a corrosive potential. The cell, as mentioned earlier, does not fit the standards for permeation experiments based on design, and since this data will only be used for this specific cell this polarization rate was not considered as a great concern.

(a) Full view **(b)** Section view

Figure 48: Design of top cell

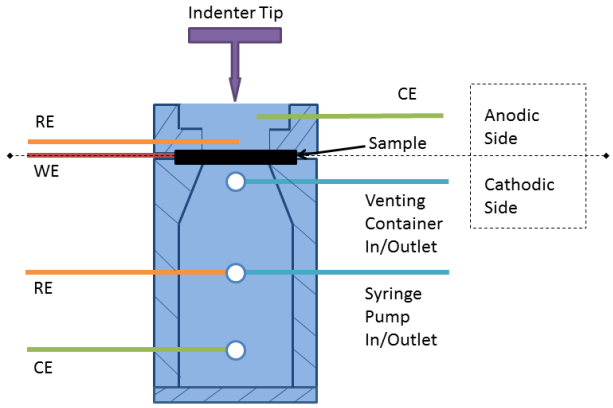

Figure 49: Setup with two-sided charging

4.11.1 Results

To see the relationship between the anodic and cathodic charging both are given in figure 50. The individual data can be found in Appendix A.

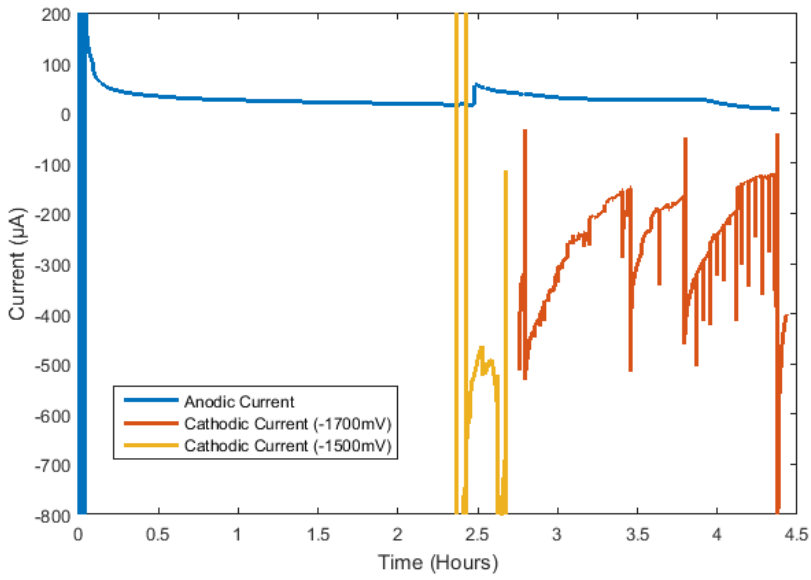

Figure 50: Anodic and Cathodic Current

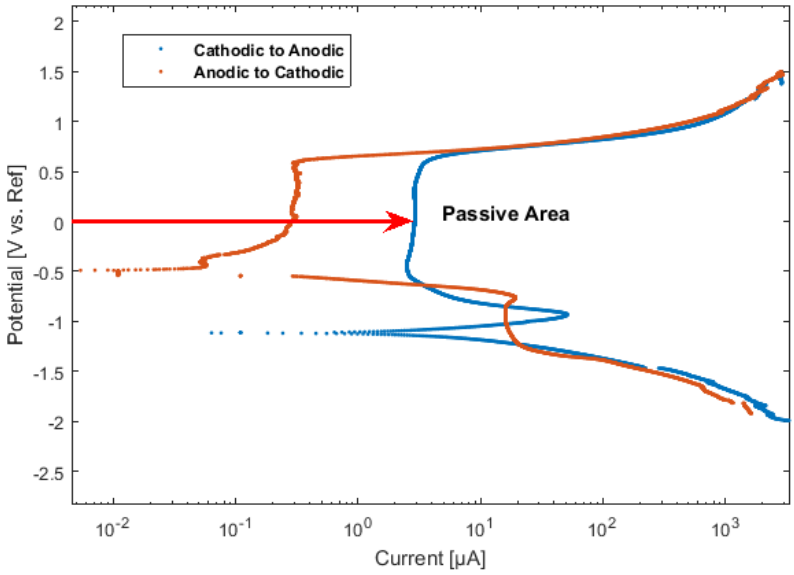

Figure 51: Polarization curve of Fe3%Si sample in custom permeation cell. Potential [V vs. Hg/Hg_2SO_4]

4.11.2 Discussion and Conclusion

The surface of the sample after the test showed some color difference on the anodic side, this is most likely an oxide layer caused by the fluctuation in the current at the beginning of the experiment as seen in figure 50. This fluctuation was due to a bubble trapped in the reference electrode inlet and as soon as this was removed the current stabilized and started to gradually decrease as expected. The cathodic side of the sample had no visible changes on the surface after testing.

When the cathodic charging started after approximated 2.3 hours of discharging the sample the anodic current barely changed. However, at 2.5 the anodic current suddenly started to increase rapidly, in a period where the cathodic current was relatively steady at -500μA. Why this sudden change appeared is unknown, but it is most likely not due to hydrogen since an increase in current due to hydrogen usually develops over time as seen in previous work [5]. The change in cathodic potential after 2.7 hours did not seem to have any effect on the anodic current and it kept decreasing towards zero in the remaining 2 hours of charging. The cathodic current did however also decrease due to the accumulation of hydrogen bubbles on the cathodic surface, hindering the electrolyte access to the surface and can be contributing factor the the decrease on the anodic

side. A measure to counter this was by manually pushing electrolyte onto the sample, similar to previous experiments. This increased the cathodic current negatively, but over time the current decreased, similar to what had been seen for other charging procedures performed with this cell.

Based on the polarization curve the current in the passive area should be in the range of 5μA after cathodic charging and approximately 0.5μA after anodic charging. This reduction in current between the two charging processes could be due to the forming and removal of oxide layers. The layers can have different conductive abilities based on if they are created after exposure to air, cathodic charging in electrolyte or anodic charging in electrolyte. Neither of these currents do however correspond to the current obtained during the two hours of discharging prior to hydrogen charging. The current can be seen in figure 50 and in appendix A, figure 56 and show a current which decreases from 160μA towards the background current. When the cathodic charging start the anodic current had stabilized around 20μA, far above the polarization currents measured. This could indicate that the time spent to discharge the sample was not long enough in order to find the background current or that the environment in which the anodic charging is ongoing is not stable. The latter could be due to the oxide layer created on the sample at the beginning of the test, or due to the open cell environment which is only found on this side of the cell to allow access to the sample.

It is, based on this information, difficult to say anything about the cell's ability to produce hydrogen and diffuse this through the sample. To test this further a suggestion is to polarize the anodic side before discharging and stopping it on the path from anodic charging to cathodic charging when the potential reaches zero. By doing this one can hopefully remove some of the oxide layer created by exposure to the air. In addition to this, the anodic (top part) of the cell should be covered to avoid as much effect of the surrounding environment as possible. If the covering solution includes a lid which completely seals the top cell it could allow for horizontal charging. If the lid in addition is easy to remove without taking the cell apart one could perform nanoindentation after charging if this is a desire and maybe even look to the possibility of horizontal nanoindenation. Unfortunately, due to a the time limit of this project work, these improvements and tests will not be done for this thesis.

5 Conclusion

The main task of this thesis was to determine if the new approach for investigating hydrogen effect at nanoscale has merit. By moving the electrolyte from the indentation surface, to the underside of the sample the hydrogen effect alone should be the only contributing factor to a possible change in nanoindentation results during hydrogen charging. As mentioned in the introduction, one of the changes which have been highlighted in previous research is the change in pop-in load. Test 7 was however a good example of how much the pop-in load could change based on the location within on single grain for Fe3%Si. Based on this knowledge and the problems with reproducing change in pop-in load after charging, this measure of change will most likely not be useful for this material and specific approach. It is however important to note that other material might behave differently regarding the pop-in.

Based on the results obtained from the in situ nanoindentation in this thesis it is unclear if this approach enables hydrogen effect measurements. Fe3%Si was the only material which was thoroughly tested due to a lack of reproducible changes. For this material the indentation depth was approximately 200nm and pop-in occurred at 20-30nm. How high the hydrogen concentration is at these locations is difficult to determine, but calculation based on previous work indicate very low concentrations compared to the concentrations on the cathodic side. More research should be put into the work of determining a critical hydrogen concentration in order to choose proper sample thickness, indentation depth and cathodic current.

The microindentation approach also raises the question of hydrogen concentration at a specific indentation depth. Although the concentration was assumed to be much higher due to deeper penetration the results did not indicate any hydrogen effect. The attempts at microindentation experiments through this thesis are however very few and both include several margins of error and the technique can not be discarded on the basis of this thesis alone.

With regards to the use of silicone oil the testing shows that for Fe3%Si samples there is no short or long term effect of the oil on the sample surface nor the indentation results. If it is a good approach to contain the hydrogen within the sample to avoid recombination on the anodic side is however less clear. No visible hydrogen bubbles were seen during charging, but by using the see through anodic top created for full permeation experiments the hydrogen bubbles, if present, will be easier to identify. There was however also not measured any hydrogen effect when the oil was used, except for in test 5. The results in test 5 were not reproduced in later experiment and are thereby rather the exception than the norm and say little about the benefits of using the silicone oil.

The full permeation experiment did not manage to prove that hydrogen was diffusing through the sample during charging from the underside. There was however discovered some areas of improvements which could be implemented to investigate this further, such as sealing the anodic cell and polarizing the cell before discharging and charging. Based on all this one can conclude that the approach which has been used is not applicable for the thick samples utilized, even if the diffusion of hydrogen is happening. The indentation depth which is reached with nano- and microindentation compared to the sample thickness gives a hydrogen concentration too low to create any effect which is measurable at the indentation site with the common cathodic hydrogen concentrations. To use this approach it is crucial to obtain a higher hydrogen concentration at the specific indentation and pop-in depth in order to say anything about the effect of hydrogen.

5.1 Further Work

- Perform further testing of the full permeation cell to determine if there is hydrogen diffusion through the sample during cathodic charging. Improvements such as sealing the anodic cell and polarazing the anodic side before discharging and charging should be tested.
- Estimation of a critical hydrogen concentration needs to be determined. One can base the estimation firstly on experiments where changes have been observed and look to the concentrations which have been presented. By adjusting the thickness one can also find the critical hydrogen concentration if no experimental data from other sources can contribute with the estimation.
- Adjust parameters such as sample thickness, electrolyte, charging current etc. in order to obtain a critical hydrogen concentration at the indentation depth and perform similar experiments as described in the thesis.
- Test a variety of materials to determine if the possible effect is easier to detect in materials with different diffusion rate and solubility as well as oxide forming materials to reduce the recombination rate.

References

[1] A. Barnoush, *Hydrogen Embrittlement, Revisited by in Situ Electrochemical Nanoindentation*. Saarbrücker Reihe Materialwissenschaft und Werkstofftechnik, Shaker, 2009.

[2] G. Stenerud, R. Johnsen, J. S. Olsen, J. He, and A. Barnoush, "Effect of hydrogen on dislocation nucleation in alloy 718," *International Journal of Hydrogen Energy*, pp. –, 2017.

[3] T. Hajilou, Y. Deng, B. R. Rogne, N. Kheradmand, and A. Barnoush, "In situ electrochemical microcantilever bending test: A new insight into hydrogen enhanced cracking," *Scripta Materialia*, vol. 132, pp. 17 – 21, 2017.

[4] E. Fallahmohammadi, F. Bolzoni, and L. Lazzari, "Measurement of lattice and apparent diffusion coefficient of hydrogen in {X65} and {F22} pipeline steels," *International Journal of Hydrogen Energy*, vol. 38, no. 5, pp. 2531 – 2543, 2013.

[5] M. S. B. Hope, "Effect of plastic deformation and microstructure on hydrogen diffusion in steel," Master's thesis, Norwegian University of Science and Technology, 2015.

[6] A. Barnoush and H. Vehoff, "Recent developments in the study of hydrogen embrittlement: Hydrogen effect on dislocation nucleation," *Acta Materialia*, vol. 58, no. 16, pp. 5274 – 5285, 2010.

[7] W. H. Johnson, "On some remarkable changes produced in iron and steel by the action of hydrogen and acids," *Nature*, vol. 11, pp. 393–393, mar 1875.

[8] M. Hirscher, ed., *Handbook of Hydrogen Storage*. Wiley-Blackwell, mar 2010.

[9] D. Hardie, E. Charles, and A. Lopez, "Hydrogen embrittlement of high strength pipeline steels," *Corrosion Science*, vol. 48, no. 12, pp. 4378 – 4385, 2006.

[10] A. Turnbull, "Perspectives on hydrogen uptake, diffusion and trapping," *International Journal of Hydrogen Energy*, vol. 40, no. 47, pp. 16961 – 16970, 2015. Special issue on 1st International Conference on Hydrogen Storage, Embrittlement and Applications (Hy-SEA 2014), 26-30 October 2014, Rio de Janeiro, Brazil.

[11] V. Olden, C. Thaulow, and R. Johnsen, "Modelling of hydrogen diffusion and hydrogen induced cracking in supermartensitic and duplex stainless steels," *Materials & Design*, vol. 29, no. 10, pp. 1934 – 1948, 2008.

[12] A. Turnbull, "Hydrogen diffusion and trapping in metals," *Gaseous Hydrogen Embrittlement of Materials in Energy Technologies*, 2012.

[13] M. Arbab and J. Hudson, "The influence of desorption kinetics on hydrogen permeation in iron," *Applied Surface Science*, vol. 29, no. 1, pp. 1 – 19, 1987.

[14] M. J. Danielson, "Use of the devanathan–stachurski cell to measure hydrogen permeation in aluminum alloys," *Corrosion Science*, vol. 44, no. 4, pp. 829 – 840, 2002.

[15] H. Hänninen, "6.01 - stress corrosion cracking," in *Comprehensive Structural Integrity* (I. Milne, R. Ritchie, and B. Karihaloo, eds.), pp. 1 – 29, Oxford: Pergamon, 2003.

[16] "G 148 – 97 standard practice for evaluation of hydrogen uptake, permeation, and transport in metals by an electrochemical technique," 2003.

[17] X. Li, Y. Wang, P. Zhang, B. Li, X. Song, and J. Chen, "Effect of pre-strain on hydrogen embrittlement of high strength steels," *Materials Science and Engineering: A*, vol. 616, pp. 116 – 122, 2014.

[18] J. Song and W. Curtin, "A nanoscale mechanism of hydrogen embrittlement in metals," *Acta Materialia*, vol. 59, no. 4, pp. 1557 – 1569, 2011.

[19] M. P. Puls, *The Effect of Hydrogen and Hydrides on the Integrity of Zirconium Alloy Components*. Springer-Verlag London, 2012.

[20] K. Herrmann, *Hardness Testing: Principles and Applications*. ASM International, 2011.

[21] "Iso 6507: Metallic materials – vickers hardness test – part 1: Test method," 2005.

[22] MitutoyoCorporation, *HM-200 Series Micro Vickers Hardness Testing Machine User's Manual*.

[23] A. C. Fischer-Cripps, *Nanoindentation*. Springer New York, 2011.

[24] A. J. Haq, P. Munroe, M. Hoffman, P. Martin, and A. Bendavid, "Effect of coating thickness on the deformation behaviour of diamond-like carbon–silicon system," *Thin Solid Films*, vol. 518, no. 8, pp. 2021 – 2028, 2010.

[25] S.-R. Jian, C.-H. Tasi, S.-Y. Huang, and C.-W. Luo, "Nanoindentation pop-in effects of bi2te3 thermoelectric thin films," *Journal of Alloys and Compounds*, vol. 622, pp. 601 –

605, 2015.

[26] A. Barnoush, N. Kheradmand, and T. Hajilou, "Correlation between the hydrogen chemical potential and pop-in load during in situ electrochemical nanoindentation," *Scripta Materialia*, vol. 108, pp. 76 – 79, 2015.

[27] A. Barnoush and H. Vehoff, "In situ electrochemical nanoindentation: A technique for local examination of hydrogen embrittlement," *Corrosion Science*, vol. 50, no. 1, pp. 259 – 267, 2008.

[28] M. Kupka, K. Stepień, and K. Nowak, "Studies on hydrogen diffusivity in iron aluminides using the devanathan–stachurski method," *Journal of Physics and Chemistry of Solids*, vol. 75, no. 3, pp. 344 – 350, 2014.

[29] M. W. Haga and S. Fossheim, "Design and manufacturing of a prototype mini hydrogen permeation cell for advanced nanomechanical testing," tech. rep., NTNU, 2016.

[30] "Standard test method for vickers hardness of metallic materialls," 1997.

[31] B. H. Lim, H. S. Hong, and K. S. Lee, "Measurements of hydrogen permeation and absorption in zirconium oxide scales," *Journal of Nuclear Materials*, vol. 312, no. 2–3, pp. 134 – 140, 2003.

Appendix A

Charging Data Test 4

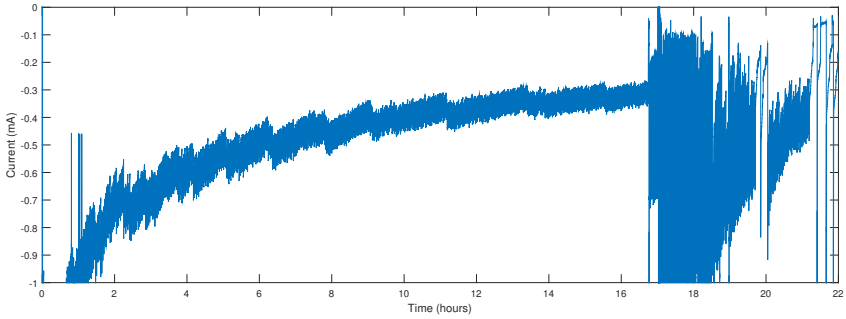

Figure 52: Charging current data from test 5

Charging Data Test 6

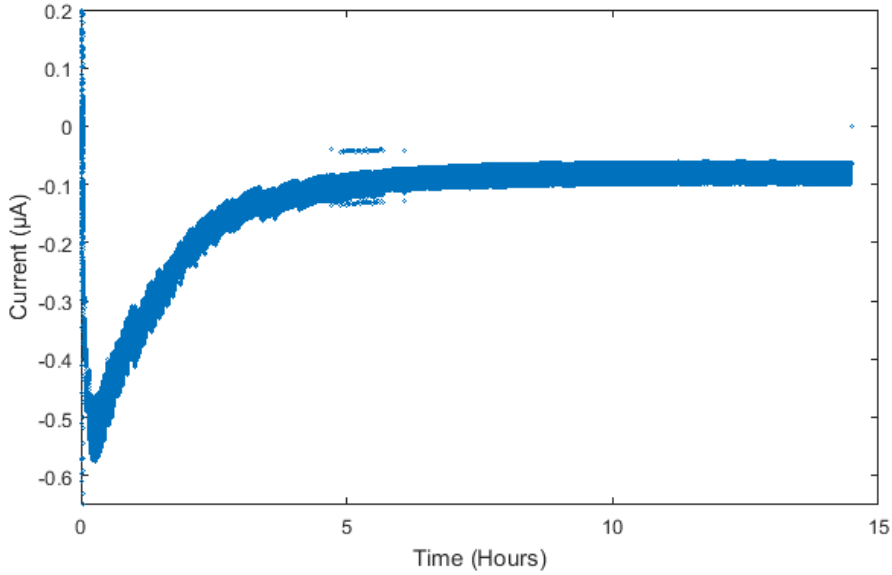

Figure 53: Charging data for test 6

Charging Data Test 7

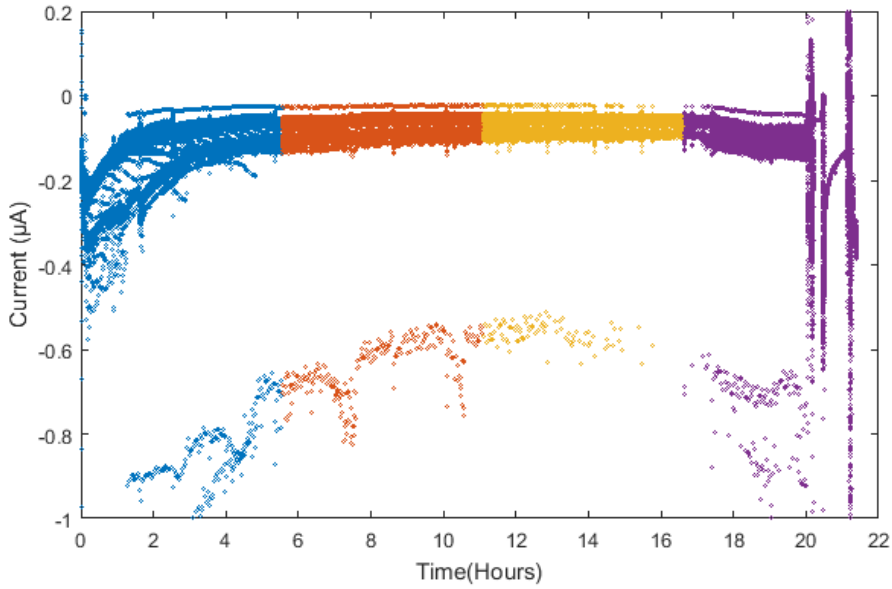

Figure 54: Charging data for test 7

Charging Data Test 9

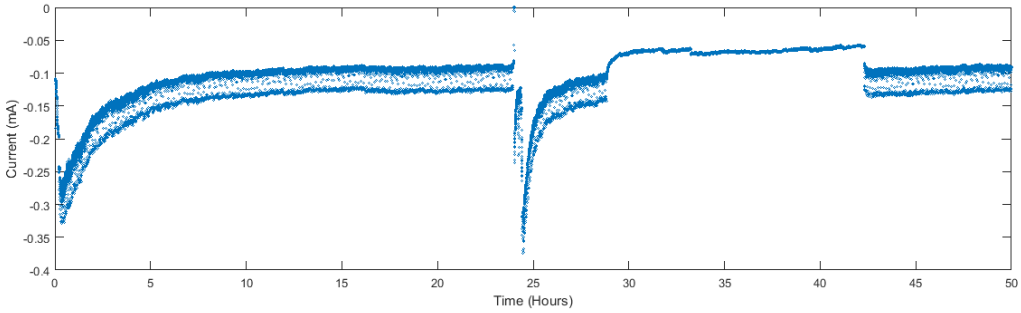

Figure 55: Charging data before microindentations for test 9

Charging Data Test 11

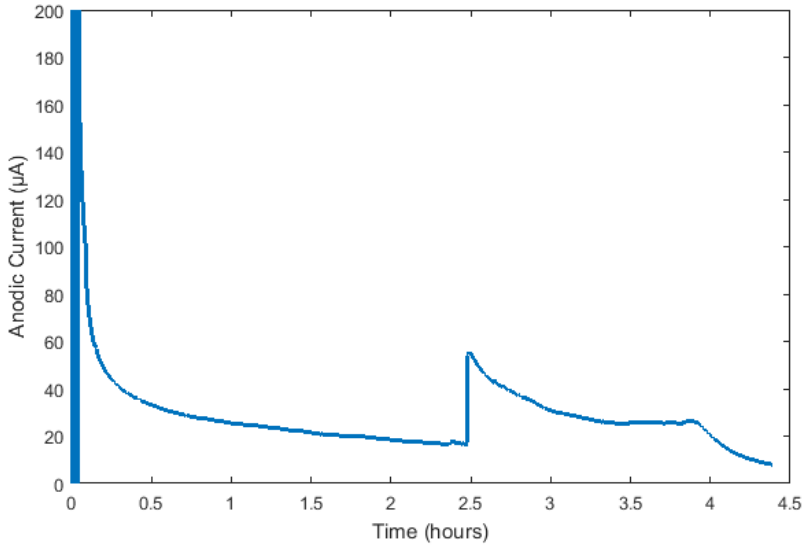

Figure 56: Anodic Current, test 11

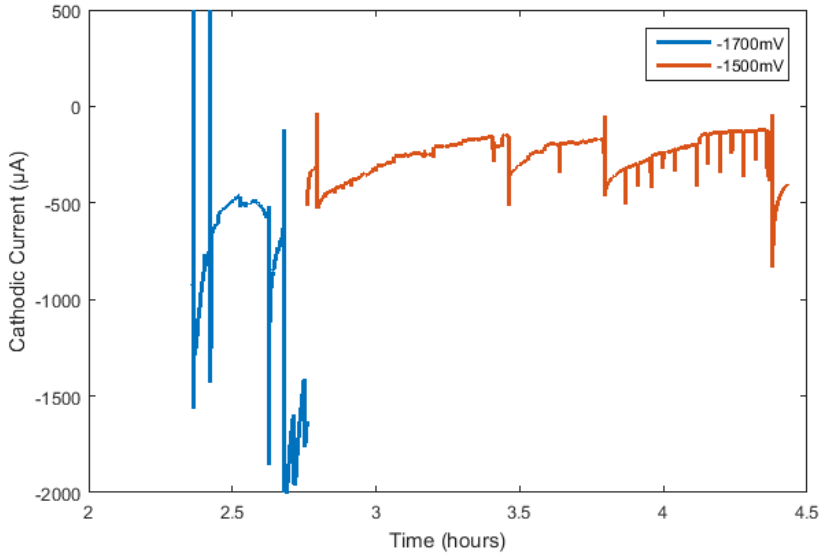

Figure 57: Cathodic Current, test 11

Appendix B

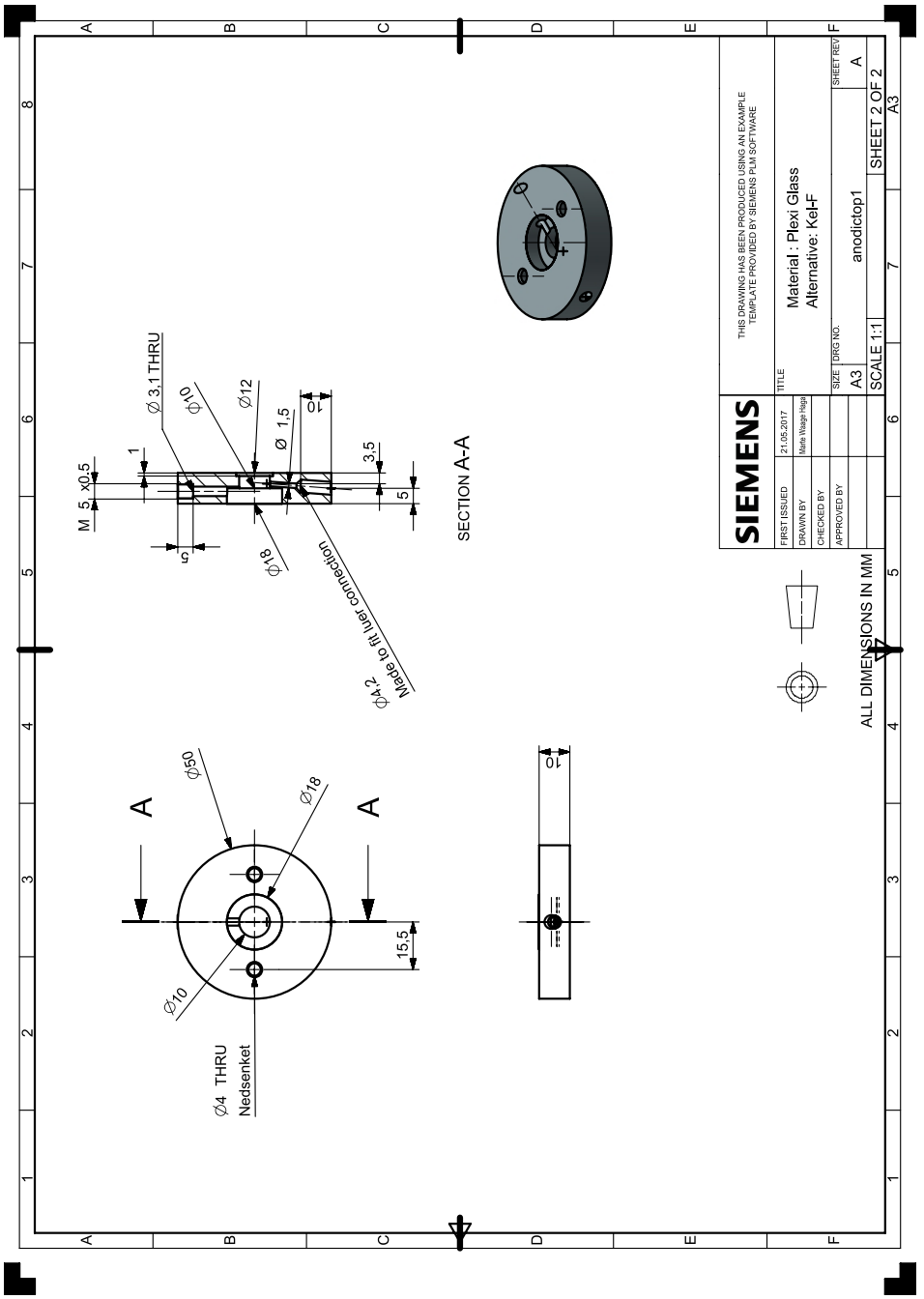
SIEMENS
THIS DRAWING HAS BEEN PRODUCED USING AN EXAMPLE TEMPLATE PROVIDED BY SIEMENS PLM SOFTWARE
FIRST ISSUED 21.05.2017
DRAWN BY Mats Waage Hagø
CHECKED BY
APPROVED BY
TITLE
Material : Plexi Glass
Alternative: Kel-F
SIZE A3
DRG NO. anodictop1
SHEET REV A
SCALE 1:1
SHEET 2 OF 2 A3
ALL DIMENSIONS IN MM
SECTION A-A
M 5 x0,5
1
Ø 3,1 THRU
Ø10
Ø12
Ø 1,5
5
3,5
5
5
Ø18
Made to fit luer connection
Ø4,2
Ø50
Ø18
Ø10
15,5
Ø4 THRU
Nedsenket
10

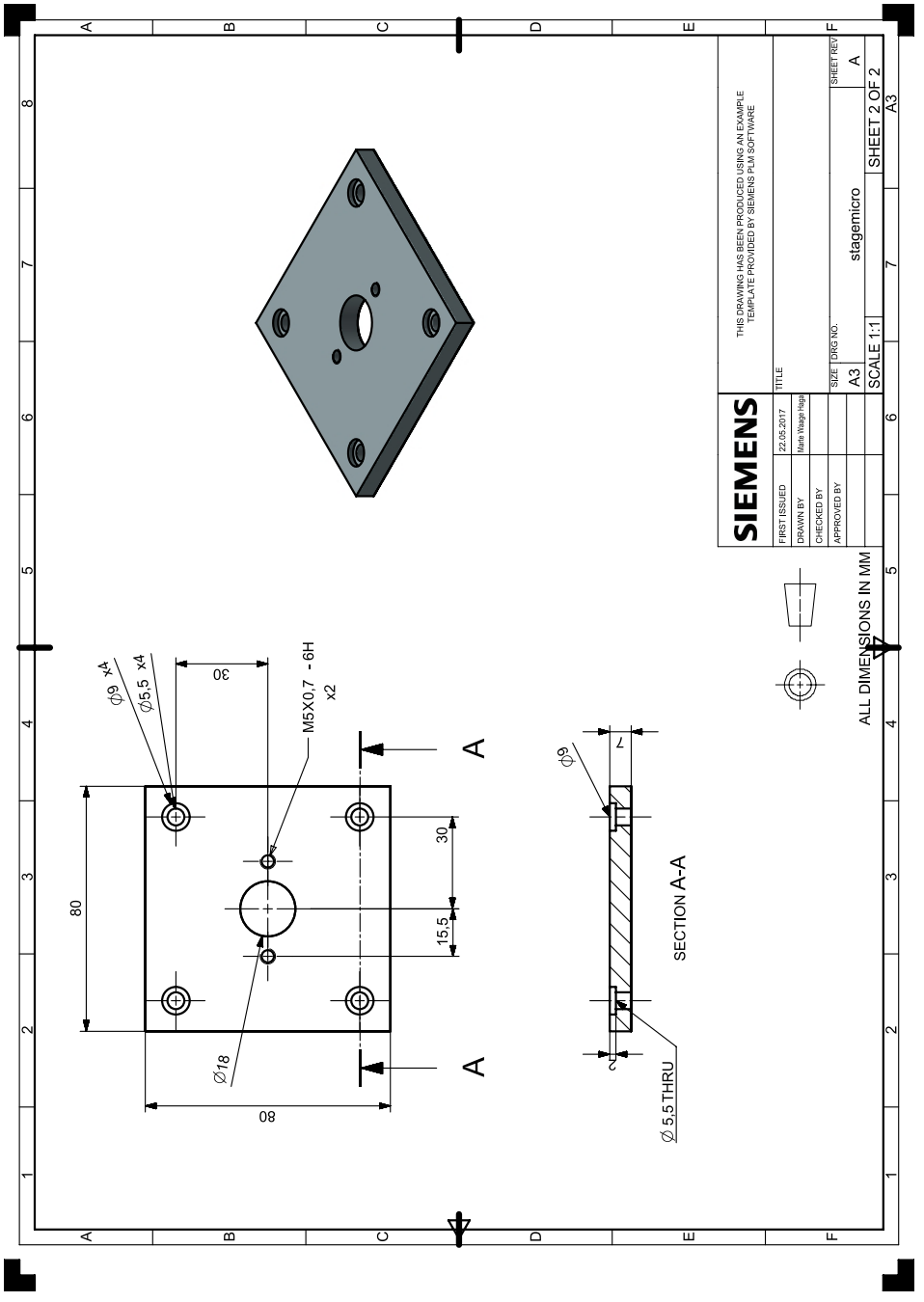
SIEMENS
THIS DRAWING HAS BEEN PRODUCED USING AN EXAMPLE TEMPLATE PROVIDED BY SIEMENS PLM SOFTWARE
FIRST ISSUED 22.05.2017
DRAWN BY Mahir Yılmaz Hoşgör
CHECKED BY
APPROVED BY
TITLE
SIZE A3
DRG NO.
stagemicro
SHEET REV A
SCALE 1:1
SHEET 2 OF 2
A3
ALL DIMENSIONS IN MM
ϕ9 x4
ϕ5,5 x4
30
M5X0,7 - 6H
x2
80
30
15,5
∅18
80
A
A
ϕ9
7
SECTION A-A
∅ 5,5 THRU

Appendix C

VEILEDER : AFROOZ BARNOUSH

Detaljert Risikorapport

ID	16839	**Status**	**Dato**
Risikoområde	Risikovurdering: Helse, miljø og sikkerhet (HMS)	Opprettet	13.01.2017
Opprettet av	Marte Waage Haga	Vurdering startet	13.01.2017
Ansvarlig	Marte Waage Haga	Tiltak besluttet	
		Avsluttet	13.01.2017

Risk assessment for in situ electrochemical nanoindentation

Gyldig i perioden:

1/13/2017 - 6/11/2017

Sted:

Nanomechanical Lab

Mål / hensikt

Perform in situ electrochemical nanoindentation experiments to examine hydrogen embrittlement

Bakgrunn

The risk assessment is used to identify possible risks related to using the nanoindenter and the chemicals in the permeation cell. This is rutine procedure for a master/project thesis at NTNU.

Beskrivelse og avgrensninger

The testing will be performed in the nanomechanical lab at Perleporten.

Forutsetninger, antakelser og forenklinger

There will be given training in using the nanoindenter and a test will be given to ensure one is capable of handling the equipment alone before individual testing can begin. Training regarding safe handling of the electrolyte has been given earlier.

Vedlegg

[Ingen registreringer]

Referanser

[Ingen registreringer]

Oppsummering, resultat og endelig vurdering

I oppsummeringen presenteres en oversikt over farer og uønskede hendelser, samt resultat for det enkelte konsekvensområdet.

Farekilde: **Unsatisfactory knowledge**

Uønsket hendelse: **Damage to equipment**

Konsekvensområde: Materielle verdier Risiko før tiltak: Risiko etter tiltak:

Endelig vurdering

If training and testing of personell handling the equipment, in this case only one person, is sufficiently executed and the person succeeds to prove the capability of operating the equipment to a satisfactory level the risk of damaging the equipment is very low. This requires that both training and testing personell commit to the training and always consider the risk while operating.

Oversikt involverte enheter og personell

En risikovurdering kan gjelde for en, eller flere enheter i organisasjonen. Denne oversikten presenterer involverte enheter og personell for gjeldende risikovurdering.

Enhet /-er risikovurderingen omfatter

- NTNU

Deltakere

[Ingen registreringer]

Lesere

[Ingen registreringer]

Andre involverte/interessenter

[Ingen registreringer]

Følgende akseptkriterier er besluttet for risikoområdet Risikovurdering: Helse, miljø og sikkerhet (HMS):

Helse	Materielle verdier	Omdømme	Ytre miljø
			

Oversikt over eksisterende, relevante tiltak som er hensyntatt i risikovurderingen

I tabellen under presenteres eksisterende tiltak som er hensyntatt ved vurdering av sannsynlighet og konsekvens for aktuelle uønskede hendelser.

Farekilde	Uønsket hendelse	Tiltak hensyntatt ved vurdering
Unsatisfactory knowledge	Damage to equipment	Training

Eksisterende og relevante tiltak med beskrivelse:

Training
There will be given sufficient training and guidance before individual use of the equipment is permitted.

Risikoanalyse med vurdering av sannsynlighet og konsekvens

I denne delen av rapporten presenteres detaljer dokumentasjon av de farer, uønskede hendelser og årsaker som er vurdert. Innledningsvis oppsummeres farer med tilhørende uønskede hendelser som er tatt med i vurderingen.

Følgende farer og uønskede hendelser er vurdert i denne risikovurderingen:

- **Unsatisfactory knowledge**
  - Damage to equipment

Oversikt over besluttede risikoreduserende tiltak med beskrivelse:

Unsatisfactory knowledge (farekilde)

No or little training is given and personell operate without the necessary knowledge and training.

Unsatisfactory knowledge/Damage to equipment (uønsket hendelse)

Wrong use of the equipment can lead to costly damage of the equipment.

Samlet sannsynlighet vurdert for hendelsen: Svært lite sannsynlig (1)

Kommentar til vurdering av sannsynlighet:

[Ingen registreringer]

Vurdering av risiko for følgende konsekvensområde: Materielle verdier

Vurdert sannsynlighet (felles for hendelsen): Svært lite sannsynlig (1)

Vurdert konsekvens: Middels (2)

Kommentar til vurdering av konsekvens:

[Ingen registreringer]

Oversikt over besluttede risikoreduserende tiltak:

Under presenteres en oversikt over risikoreduserende tiltak som skal bidra til å reduseres sannsynlighet og/eller konsekvens for uønskede hendelser.

Oversikt over besluttede risikoreduserende tiltak med beskrivelse: